

Tripolar Concentric Ring Electrode Brain Computer Interfacing with Real and Imagined Movements

By

Joshua Barclay

*Thesis
Submitted to Flinders University
for the degree of*

**Bachelor of Engineering (Biomedical)(Honours),
Master of Engineering (Biomedical)**

College of Science and Engineering
October 16, 2023

TABLE OF CONTENTS

TABLE OF CONTENTS	I
ABSTRACT	III
DECLARATION	IV
ACKNOWLEDGEMENTS	V
LIST OF FIGURES	VI
LIST OF TABLES	VII
INTRODUCTION	1
Background	1
Neurodegenerative Diseases	1
Brain Computer Interfaces	1
Tripolar Concentric Ring Electrodes.....	3
Project Details	4
Aim	4
Research Questions	4
Scope	4
Thesis Structure.....	5
LITERATURE REVIEW	6
Orientation.....	6
Measuring Brain Signals.....	6
Electroencephalography	6
Tripolar Concentric Ring Electrodes.....	7
Experimental Paradigms	8
P300 Event related Potential.....	8
Steady-State Visually Evoked Potential	9
Motor Imagery and Sensorimotor Rhythms.....	10
Classification	11
Support Vector Machines.....	11
Artificial Neural Networks.....	12
Gap Statement	13
METHODOLOGY	14
Experimental Design	14
Participants.....	14
EEG Electrode Configuration	14
EMG Electrode Configuration	16
Experimental Protocol	17
Motor Imagery Paradigm	17
EEG Signal Processing.....	18
EMG Signal Processing.....	19

Classification	19
Electrode Selection	19
Support Vector Machine	20
Neural Network.....	21
RESULTS.....	23
Event Related Desynchronisation.....	23
Emulated EEG	23
tCRE EEG	27
Classification	29
Support Vector Machine	29
Neural Network.....	30
DISCUSSION	32
Comparison With Literature.....	32
Experimental Protocol.....	32
Event Related Desynchronisation	32
Classifier Performance.....	34
Future Work	36
PROJECT OUTCOMES	37
Conclusion	37
BIBLIOGRAPHY	39
APPENDICES	43
Appendix A.....	43
Check Desynchronisation Script	43
Appendix B.....	44
Class Rebalance Script.....	44
Appendix C.....	45
Create Segments Function	45
Appendix D.....	46
Training Dataset Creation Script	46

ABSTRACT

Neuromuscular disorders such as multiple sclerosis or motor neuron disease lead to long-term degeneration of the efferent nervous system, resulting in progressive loss of motor function. Loss of motor function has been shown to severely impact independence and quality of life. As the underlying mechanisms triggering neuromuscular disorders are poorly understood, treatment focuses on improving patient independence and quality of life with assistive technologies. Brain computer interfaces (BCI) are a type of assistive technology that allow users to interact with exterior devices using brain activity alone, being particularly suited for patients with limited motor function. Many types of 'paradigm' can be used to evoke specific patterns in the brain, which can be used to control a brain computer interface. The motor imagery paradigm is one type, which requires the user to imagine a movement, triggering an event related desynchronisation (ERD) to occur within the relevant region of the sensorimotor cortex. Motor imagery paradigms are advantageous in that they allow intuitive control of a brain computer interface through self-modulation of their brain activity. Despite this, the current literature reports poor performance due to higher training requirements and reported BCI illiteracy. The proposed method was a modified motor imagery paradigm, which used real and imagined movements to train a classifier. Using EEG and EMG, event related desynchronisation was to be measured and recorded across movements, for use in training support vector machine and neural network classifiers. By using tripolar concentric ring electrodes (tCRE) as the sensory modality, it was hypothesised that this would reduce the presence of muscle artefacts, improving classifier training outcomes. Participants for the study were recruited from within the research group ($n = 7$). Participants were tasked with performing a series of movements, classified as either full extension, partial extension and imagined extension of the fingers. All participants demonstrated some level of event related desynchronisation using both emulated EEG and tCRE. From the channel demonstrating the greatest desynchronisation in each participant, a dataset was created for classifier training. A support vector machine was trained using leave-one-sample-out cross-validation, with a reported classification accuracy of $(66.8\% \pm 3.71)$ and $(65.6\% \pm 1.69)$ for emulated EEG and tCRE, respectively. Similarly, a neural network was trained using K-fold cross-validation, returning an emulated EEG accuracy of $(51.7\% \pm 1.01)$ and tCRE accuracy of $(52.7\% \pm 0.90)$. The results indicate that tCRE offers no additional benefit to classifier performance over emulated and ordinary EEG. Comparing with the literature, it was noted that studies utilising similar methods achieved higher classifier accuracy. It was speculated that this discrepancy was a result of the number of channels used for training the classifier. Support vector machine training was repeated, including all channels, with a reported accuracy of 88%, providing support for this speculation. Future studies should investigate the relationship between channel number and classifier performance further, particularly focusing on methods that maintain performance with a reduced channel setup.

DECLARATION

I certify that this thesis:

1. does not incorporate without acknowledgment any material previously submitted for a degree or diploma in any university
2. and the research within will not be submitted for any other future degree or diploma without the permission of Flinders University; and
3. to the best of my knowledge and belief, does not contain any material previously published or written by another person except where due reference is made in the text.

Signature of student.....

Print name of student..... Joshua Barclay

Date..... 16/10/2023

I certify that I have read this thesis. In my opinion it is/is not (please circle) fully adequate, in scope and in quality, as a thesis for the degree of Engineering (Biomedical) (Honours)/ Master of Engineering (Biomedical). Furthermore, I confirm that I have provided feedback on this thesis and the student has implemented it minimally/partially/fully (please circle).

Signature of Principal Supervisor.....

Print name of Principal Supervisor..... A/Prof. Kenneth Pope

Date..... 16/10/2023

ACKNOWLEDGEMENTS

I would like to thank A/Prof Kenneth Pope for being my supervisor through this project. Your feedback and guidance throughout my project have been incredibly beneficial, both to the quality of my work and to the way I tackle problems. Thank you for teaching me how to collect EEG data (even though it never seemed to work on you) and for teaching me the wonderful tools of MATLAB (it's not so bad after all). Thank you for your humour, support and understanding throughout the year and for putting up with my 'idiosyncratic eccentricities'.

Thank you to Katelyn Large for always being there for me when I was struggling through my project and helping me sound through ideas. I'm really glad you were always bugging me about my project, keeping me on track whenever I had trouble focusing (my project thanks you too). Thank you especially for always cheering me up when I was feeling down or making me laugh when I was stressed. Your presence in my life is a positive boon that I'm perpetually grateful for, and I look forward to spending time with you for many years to come.

I would also like to thank the entire research group for being exceptionally helpful throughout my project, and for volunteering their brains for data collection. You've all been kind, funny and supportive throughout the stressful periods of this years. It's been absolute pleasure to work with all of you.

LIST OF FIGURES

Figure 1 Comparison of tCRE and disc electrodes.....	8
Figure 2 Representation of event related desynchronisation.....	10
Figure 3 The CREmedical t-interface 20.....	15
Figure 4 EEG montage of the experimental setup in accordance with the 10/5 system.....	16
Figure 5 Target movements performed as part of the experimental protocol.....	17
Figure 6 Layout of each video prompt.....	18
Figure 7 Annotated layout of each video prompt for generation of training samples.....	20
Figure 8 Leave-one-sample-out cross validation.....	21
Figure 9 K-fold cross validation.....	22
Figure 10 Mu frequency band activity for participant 1, separated by electrode and movement..	23
Figure 11 Electromyograph activity of participant 1, averaged across epochs and separated by movement.....	24
Figure 12 Emulated EEG Group average relative mu band power, separated by electrode and movement.....	25
Figure 13 Absolute ERD group average using corresponding best channel.....	26
Figure 14 Participant 1 mu band power using tCRE, separated by electrode and movement.....	27
Figure 15 Group average relative mu band power, separated by electrode and movement..	28
Figure 16 tCRE absolute ERD group average using corresponding best channel.....	29
Figure 17 Support vector machine group average confusion matrices.....	30
Figure 18 Neural network confusion matrices for participant 1, trained on the emulated EEG (right) and tCRE (left) datasets.....	31
Figure 19 EMG activity of data outlier; participant 6.....	33
Figure 20 Confusion matrix of support vector machine performance on participant 1 using all electrodes.....	35

LIST OF TABLES

Table 1 Electrodes demonstrating the greatest change in mu band power during an event related desynchronisation, ordered by participant and sensory modality used. 20

INTRODUCTION

Background

Neurodegenerative Diseases

Neurodegenerative diseases refer to a category of conditions that result in progressive degeneration of functionality within the nervous system. A subset of these conditions can affect efferent pathways, leading to deterioration and ultimately loss of motor control.

For example, multiple sclerosis (MS) is an autoimmune disorder which leads to an individual's immune system attacking protective myelinated sheathing within the central nervous system. It is estimated that multiple sclerosis affects more than 2.8 million people worldwide (Walton *et al.* 2020). Similarly, amyotrophic lateral sclerosis (ALS) is another neurodegenerative disorder which causes degeneration of efferent neurons related to voluntary movement. ALS is considered the most common form of motor neuron disease and has an estimated prevalence of 6 per 100 000 annually (Talbot *et al.* 2016). While the mechanisms of progression differ between disease, the outcome is the same, reduced transmission of efferent signals, resulting in muscle weakness and eventual loss of voluntary motor control.

The progression of multiple sclerosis and other neurodegenerative disorders has been found to have a profoundly negative effect on an individual's quality of life, with increased fatigue and loss of self-efficacy cited as dominant factors which limit quality of life (Young *et al.* 2021). Presently, the exact causes of both multiple sclerosis and amyotrophic lateral sclerosis are poorly understood, with no treatment options available to cure or halt progression (NINDS, 2023). As such, treatment typically focuses on improving both comfort and independence through the use of assistive technologies.

Brain Computer Interfaces

A brain computer interface (BCI) is a tool that allows an individual to interact with external devices through the use of brain signals. Brain computer interfaces can be divided into 3 subsystems; a sensory apparatus for detection of brain signals, a processor for producing useful instructions from brain activity, and a machine interface, which transmits instructions to an external device.

Brain computer interfaces have been developed as a communication tool primarily for use in the field of rehabilitation. For individuals with reduced capacity for muscle movement, it can be incredibly difficult to interact with the environment. Many forms of assistive interface require movement on some level, whether it be through a mechanical apparatus such as a keypad, an eye-tracker or voice commands. With advanced progression of neuromuscular disorders, it may not be possible to use these assistive tools effectively. Conversely, brain computer interfaces do not rely on physical interaction with an assistive device. Rather, BCI can be used for interaction through either conscious

or unconscious modulation of brain signals, allowing continued use throughout disease progression, even in instances of complete paralysis.

While all brain computer interfaces can be divided into the same 3 subsystems, the sensory apparatus used, as well as the types of brain signals used in controlling it can differ significantly. Sensing can be further categorised as invasive or non-invasive, where invasive methods involve the implantation of sensors below the skin, as in electrocorticography. While invasive methods can improve the ratio of signal to noise, their use may be received poorly by patients, depending on their perceived risk-reward ratio (Lahr *et al.* 2015). Conversely, this thesis focuses on the use of non-invasive electroencephalography (EEG), which monitors brain activity by adhering electrodes to the scalp. Electroencephalography is favourable over other non-invasive sensing modalities like magnetic resonance imaging (MRI), due to its portability and reduced cost (Abiri *et al.* 2018). As a result of its high temporal resolution, EEG is particularly well-suited for use in real-time control, an important aspect of BCI design.

The type of stimulation paradigm used to control a brain computer interface can be categorised as either internal or external. External stimulation involves the use of an additional external apparatus to evoke specific brain signals through visual or auditory stimulation. One popular paradigm uses a flickering light to produce steady-state visually evoked potentials (SSVEPs). By flickering a light at a specific frequency, a complementary increase in the power of this frequency can be observed in the spectral content of EEG signals (Abiri *et al.* 2018). Another type of external stimulation paradigm is the P300, which is a type of event related potential triggered through the identification of irregular visual stimuli, referred to as the 'oddball paradigm'. While external stimulation paradigms are advantageous in that the response is unconscious, and as such training time is substantially reduced, additional equipment is required to elicit the desired response.

Internal stimulation paradigms rely on the conscious modulation of brain activity to evoke the desired brain signal. This thesis focuses on the use of an internal stimulation paradigm, specifically the motor imagery paradigm. Previous literature has demonstrated that the conscious imagination of movement activates the same areas of the brain responsible for generating real movement (Pfurtscheller *et al.* 1997). During moments of rest within the motor cortex, neurons demonstrate synchronisation of activity within the mu frequency band from 8-12 Hz. Activation of the motor cortex during real and imagined movements triggers an 'event related desynchronisation' (ERD), in which the mu frequency band becomes reduced (Pfurtscheller *et al.* 1999). Motor imagery paradigms focus on identifying this event related desynchronisation through imagination of a specific movement. The motor imagery paradigm is advantageous over external stimulation techniques in that control is achieved consciously, removing the requirement for additional external devices.

Brain computer interfaces are currently limited within the motor imagery paradigm, as a result of a phenomenon referred to as BCI illiteracy. Illiteracy within the motor imagery paradigm is an inability

to accurately induce the correct event related desynchronisation after sufficient training, with surveys indicating between 10% and 50% of participants tested showed illiteracy (Zhang *et al.* 2021). Additionally, due to the difficulty of imagining movements, training an individual to successfully use a motor imagery BCI can take many sessions. It was hypothesised in a previous study that combining real and imagined movements together during training would make visualising imagined movements easier, decreasing training time and improving classifier performance (Ostendorf, 2022).

Tripolar Concentric Ring Electrodes

While the temporal resolution of traditional EEG is considered much better than other sensing methods like MRI, the spatial resolution of EEG is poor, limiting the localisation of brain signals. One technique for improving the spatial resolution in an EEG is to calculate the surface Laplacian, which filters spatially distant or spread signals, such as muscle noise (Koka *et al.* 2007). However, to calculate the Laplacian, a large number (64+) of electrodes is required (Kayser *et al.* 2016). While acceptable within a clinical setting, a high number of electrodes should be avoided in BCI contexts, as too many wires could make the design cumbersome and difficult to setup. Furthermore, calculating the Laplacian is a computationally intensive task, requiring increased computational power to perform in real-time.

An alternative method for improving spatial resolution is to utilise a tripolar concentric ring electrode (tCRE). A tripolar concentric ring electrode extends ordinary electrodes by including two additional rings, each located within the previous. It has been demonstrated that tCRE is capable of calculating the Laplacian automatically, reducing the presence of mutual information and noise without the requirement for cumbersome electrode setups (Koka *et al.* 2007). Furthermore, as tCRE is composed of several concentric rings, the outermost ring can be used to provide ordinary disc electrode EEG, referred to as emulated EEG (eEEG).

Project Details

Aim

This thesis is an extension of a previous project that aimed to test the validity of combining real and imagined movements to train a classifier in the motor imagery paradigm (Ostendorf, 2022). While the previous project focused on the creation of a training paradigm that used both real and imagined movements, this thesis extends the focus to determine the merits of using tCRE within this new paradigm. By utilising tripolar concentric ring electrodes, it may be possible to improve the spatial selectivity of electrodes, allowing for improved localisation of event related desynchronisation. Furthermore, by improving localisation it may be possible to use higher density electrode setups for identification of ERD in closely located regions of the motor cortex, potentially allowing for the development of a more robust BCI. To determine the suitability of tCRE in BCI applications, a series of research objectives were created:

- **RO1:** Using a motor imagery paradigm, collect EEG data with tCRE
- **RO2:** Identify the presence of event related desynchronisation within emulated EEG and tCRE EEG data
- **RO3:** Develop a support vector machine classifier for comparing emulated EEG and tCRE performance with previous work
- **RO4:** Experiment with neural network classifiers for identifying event related desynchronisation

Research Questions

With completion of the listed research objectives, the following research questions should be answered:

- **RQ1:** Can event related desynchronisation be observed using tripolar concentric ring electrodes?
- **RQ2:** What differences can be observed in event related desynchronisation between tCRE and emulated EEG?
- **RQ3:** How does training an ERD classifier on tCRE data influence accuracy, in comparison to ordinary and emulated EEG?
- **RQ4:** What differences in training performance can be observed between support vector machine and neural network algorithms?

Scope

This project is focused specifically on identifying the potential merits of tCRE over ordinary and emulated EEG in training an ERD classifier. While the project focuses on the benefits of implementation in BCI systems, the actual development of a BCI was outside of the project's scope. Additionally, the project was limited to members of the research group, so no testing on individuals with neurodegenerative disorders was conducted. Because of the individualistic nature of brain

activity, it was not feasible to create a classifier to predict ERD across participants. Instead, a separate classifier was used for each participant. Due to time constraints placed on the project, each classifier was trained on data collected from a single recording session, rather than several sessions, limiting the size of the training dataset.

Thesis Structure

This thesis is subdivided into six chapters. The literature review in chapter 2 provides additional context on the background with justifications on the major design choices of the project based on methods within the literature. The limitations of current literature were identified, with a gap statement included to show the relevance of the project and its potential contribution to the literature. The methodology in chapter 3 details the experimental protocol used during data collection, as well as highlight the data processing used. Additionally, chapter 3 includes details on the training and testing methods used for each classifier, as well as the methods used for analysing performance. Chapter 4 shows the results of the project, including graphs identifying event related desynchronisation in participant data, as well as the measured performance of each classifier across both tCRE and emulated EEG. Chapter 5 discusses the findings of the project in the context of the research questions presented and previous literature, as well as potential future directions for the project. Finally, chapter 6 highlights the key outcomes of the project, and concludes the thesis.

LITERATURE REVIEW

Orientation

Brain computer interfacing is a complex assistive technology, with substantial research dedicated to improving its many subsystems. As this project is primarily focused on the sensing and processing phases of a BCI, rather than its integration into exterior support devices, this literature review will investigate the literature relevant to the sensory modalities used, experimental paradigms for controlling the BCI, and classification techniques that have been used in BCI contexts. After summarising current knowledge in this field, a gap statement was included to highlight how this project may fill a gap in the literature.

Measuring Brain Signals

Electroencephalography

Electroencephalography (EEG) is one of the oldest and most popular sensory modalities used in the development of brain-computer interfaces. Michel and Brunet (2019) suggest that despite the portability and inexpensive nature of EEG, the modality is currently limited by the poor spatial resolution of electrodes. Similarly, Burle et al (2015) arrive at the same conclusion, while EEG is useful as a diagnostic tool for neurological activity, the lack of spatial resolution associated with the method limits the ability to localise detected activity. Burle et al follows by suggesting that EEG spatial resolution can be improved significantly by utilising the surface Laplacian technique. This is corroborated by Carvalhaes and Barros (2015) who discuss the theory and methods behind the implementation of the surface Laplacian in EEG. The surface Laplacian is a technique that relates the surface scalp potentials to the localised flow of electric current as a result of brain activity. Both Burle et al (2015) and Carvalhaes and Barros (2015) agree that approximating the surface Laplacian with EEG should significantly increase its associated resolution. Increasing the spatial resolution of EEG is advantageous in that it will allow enhanced localisation of detected signals, providing greater insight into the function of the brain. In the context of brain-computer interfaces, enhanced spatial resolution would be advantageous in that signals could be detected from closely positioned brain regions, allowing for the effective control of more advanced BCI designs. Carvalhaes and Barros (2015) state that while estimated surface Laplacians could be used for improving spatial resolution, their calculation can be computationally intensive, particularly on larger datasets. Extending this further, surface Laplacians may be too computationally intensive for implementation in portable and especially real-time systems like BCI. For use in brain-computer interfaces, a more computationally efficient method will be necessary to reap the benefits of increased resolution.

Tripolar Concentric Ring Electrodes

Tripolar concentric ring electrodes (tCRE) may offer a new method of improving EEG resolution in a computationally efficient manner. Besio et al (2006) developed a new technique for conducting EEG that utilised electrodes formed from multiple concentric rings. These tripolar concentric ring electrodes were designed to automatically calculate the surface Laplacian effectively removing the associated computation requirements of the technique. This is particularly advantageous for systems that may lack the appropriate computing power or for systems that may need to process EEG in real-time, as with BCI. Liu and Besio (2013) conducted a comparative study between disc electrodes and tCRE to determine the difference in spatial selectivity between the two sensor types. Common spatial subspace decomposition was used to extract visually evoked potentials in participants. The normalised power of the visually evoked potentials was compared between modalities, with the results indicating a significantly higher specificity for tCRE. Furthermore, the tCRE electrode demonstrated a half sensitivity volume one tenth the size of the corresponding disc electrode. A follow-up study by Liu et al (2020) corroborated these results, calculating a half sensitivity volume for disc electrodes that was 9.6 times greater than their tCRE counterpart. An earlier study by Koka and Besio (2007) found similar results, with tCRE demonstrating a significantly higher signal-to-noise ratio and reduced mutual information between electrodes. These provide support to the idea that tCRE may be suitable for use in higher density electrode setups for more advanced BCI designs. It should be noted that the validity of these results may be questionable, as one of the key researchers, Walter Besio, was heavily involved in the development and commercialisation of tCRE, and as such may have a conflict of interest in the results published. Aghaei-Lasboo et al (2020) found that the performance of tCRE and disc electrodes in seizure detection was comparable, although noting that tCRE did yield reduced muscle artifacts in the recorded signal. Besio et al (2014) also reported greater attenuation of muscle artefacts in the analysis of high-frequency oscillations occurring in epilepsy patients. It was noted that tCRE demonstrated poorer performance for the detection of signals that were widely spatially distributed. This is an implicit weakness of tCRE, as a result of the higher spatial selectivity greater attenuating signals that are further away from the electrode. Despite this apparent weakness, the advantages of automated Laplacian calculation make tCRE a suitably appropriate candidate for use in brain-computer interfacing.

Figure has been removed due to copyright restriction

Figure 1 Comparison of tCRE and disc electrodes. Tripolar concentric ring electrodes extend traditional disc electrodes by including additional electrode rings located concentrically. In comparison with disc electrodes, tCRE has its own reference and ground and is capable of calculating the Laplacian automatically, drastically reducing computational demands and improving attenuation on spatially spread signals, such as muscle artefacts. (CREmedical, 2023)

Tripolar ring electrodes have already seen some use in the development of brain-computer interfaces. Besio et al (2008) used tCRE to develop a brain-computer interface that used an autoregression model for pre-feature selection. The classifier trained using tCRE data demonstrated a 10 percent increase in accuracy; 78.73% vs 68.01% for tCRE and disc electrode classifiers, respectively, indicating that tCRE could be used successfully in BCI applications. A study by Almajidy et al (2015) utilised a multimodal recording system that combined tCRE with other sensory modalities, such as near-infrared spectroscopy. It was indicated that using a combination of different modalities together in conjunction with linear discriminant analysis yielded higher classifier accuracy (85.2%) compared to any individual system on its own. Despite offering better performance by using additional sensor types, the bulky and restrictive nature of the setup would make it unfit for use in a portable brain-computer interface. A recent study by Alzahrani and Anderson (2021) compared the performance of tCRE and disc electrodes in the development of a movement-related potential (MRP) classifier. tCRE demonstrated a 20% improvement in mean classifier accuracy, compared to the data collected from the disc electrodes. In conjunction with the other findings, it would appear that tCRE can be used effectively in developing brain-computer interfaces, with performance particularly reliant on the paradigm and classifier used.

Experimental Paradigms

P300 Event related Potential

One popular paradigm that is used in the development of brain-computer interfaces is the P300. Fabiani et al (1987) described the P300 as an event related potential that appears as a positive deviation roughly 275 milliseconds after the triggering stimulus. P300 was described as being brought on by a task-related visual stimulus. Polich (2007) discusses a method for producing a P300 in a patient, as well as differentiating between different types of P300 potentials. Polich suggests that P300 can be elicited through the oddball paradigm, wherein an irregular stimulus is included within a pattern of regular stimuli. As the irregular stimulus is identified, a P300 is produced in the

participant, with particularly significant activity in the parietal region. Polich goes further to suggest that by adding a tertiary 'distractor' stimulus to the oddball paradigm, two different types of P300 can be elicited, P3a and P3b. Since P300 can be elicited easily through the oddball paradigm, it is possible to design a brain-computer interface around this. For example, by having a set of images displayed and flashed consecutively, different BCI outputs can be activated by focusing on a corresponding image when it flashes. An early paper by Farwell and Donchin (1988) discuss an implementation of this strategy to control a rudimentary keyboard. Character rows and columns would be cycled repeatedly with a P300 being produced when the desired row or column was reached. Using this setup, it was possible to achieve a character selection rate of 2.3 per minute. Another study by Piccione et al (2006) used P300 for two-dimensional control of a ball on a screen. Arrows were placed on each side of the screen and flashed consecutively. As the arrowing being focused on is flashed, a P300 will be produced, which is used to control the direction of the ball accordingly. Bell et al (2008) used P300 as a proof-of-concept for a humanoid robot BCI. A set of images would be displayed to participants and flashed randomly, evoking a P300. A support vector machine was then used to classify which image was being focused on. Across the set of participants (n = 8), a 95% accuracy was achieved for 5-second selection windows. Comparing the three studies, it was determined that P300 is an external stimulus, meaning it relies on some external device to elicit the correct response in the subject's brain. The advantage of this is that minimal training is required for use in a brain-computer interface, since the P300 is unconsciously generated. A disadvantage of this is that the subject will be reliant on some external device to use the BCI, decreasing independence. Another disadvantage that was noted, particularly in Farwell and Donchine (1988) was the slowness of decision making. The P300 will only be produced by looking out for a particular stimulus, meaning that the speed of control is limited by how fast each stimulus can be cycled. It was also noted that consistent usage of the oddball paradigm may make the stimulus 'expected', reducing the magnitude of the P300 with time. The slow operation time, in conjunction with the reliance on external stimulus make the P300 a poor choice as a paradigm for a mobile brain-computer interface.

Steady-State Visually Evoked Potential

Steady-state visually evoked potentials (SSVEPs) are another popular paradigm used in the control of brain-computer interfaces. Vialette et al (2010) describes an SSVEP as a type of visually evoked potential related to a flickering visual stimulus. With the introduction of a flickering light stimulus, a frequency is induced in the brain complementary to the frequency of the flicker. This is beneficial for BCI in that many different flicker rates can be used, allowing for more complex control of a device. It was noted that for lower frequency stimuli, the light flicker could cause noticeable eye fatigue for the participant, providing a significant disadvantage for using SSVEP. Similarly, both Chang et al (2014) and Müller et al (2011) reported subject eye fatigue from stimulus flicker. To reduce fatigue, Chang et al used a higher frequency amplitude-modulated carrier signal to display lower frequency signals.

This achieved similar performance to lower frequency SSVEPs, while minimising patient discomfort. Similarly, Müller et al utilised a 37-40Hz stimulus to still elicit an SSVEP, while reducing subject fatigue. Volosyak et al (2011) used high frequency SSVEPs with participants at a fair to control a robot through a maze. Despite being used in an area with significant environmental noise, most participants were still able to use the BCI. This is an advantageous trait, since most BCIs will be used outside of a controlled clinical setting. Like the P300, steady-state visually evoked potentials are produced by external stimulus and are not produced consciously. Vialette et al suggests that more than 90% of users are capable of operating an SSVEP brain-computer interface with no prior experience. The primary disadvantage of using SSVEP for a brain-computer interface is the requirement of a visual display to elicit the SSVEP, which may limit the device's mobility and the user's independence. As such, a paradigm that is not reliant on an external stimulus would be preferable for developing a brain-computer interface.

Motor Imagery and Sensorimotor Rhythms

Motor imagery paradigms or sensorimotor rhythms offer an alternative to visually evoked potentials that can be used in brain-computer interfaces. Abiri et al (2019) describes motor imagery as imagining a movement without necessarily initiating the movement physically. Pfurtscheller and Neuper (1997) investigated the effect of motor imagery on the primary sensorimotor area, finding that imagined movement produces a short-lasting localised desynchronisation, seen in figure 2. It was noted that the region of desynchronisation correlates with the same regions that desynchronise during voluntary movement.

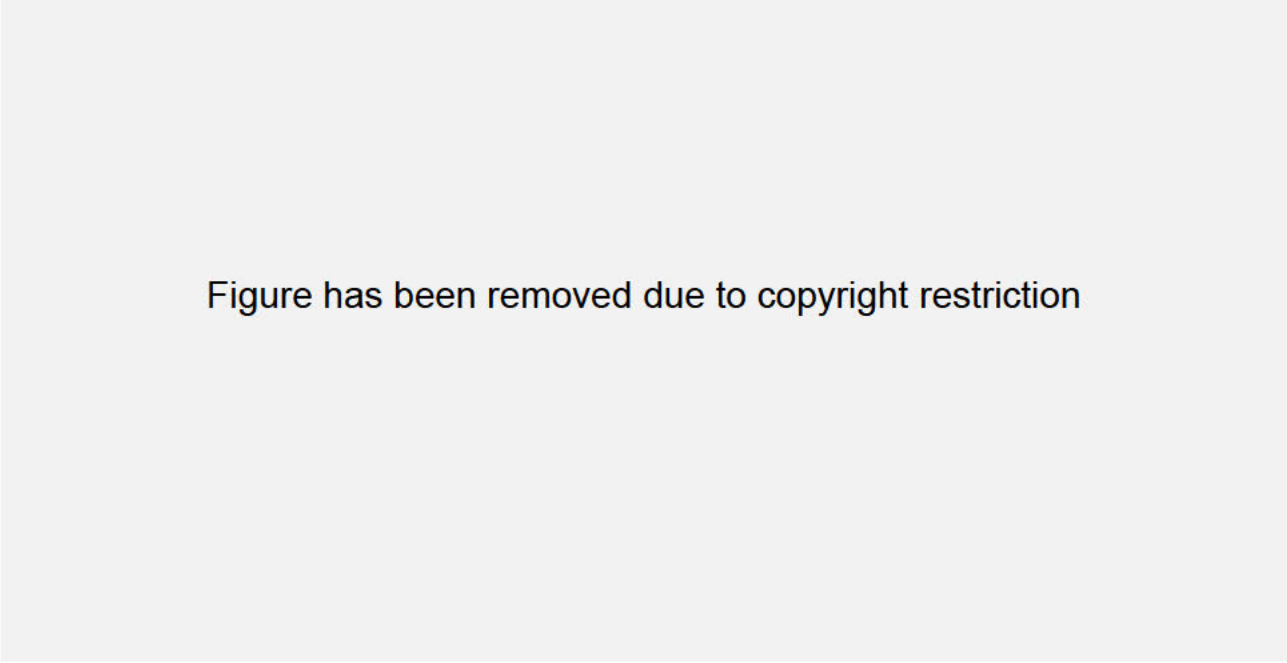


Figure has been removed due to copyright restriction

Figure 2 Representation of event related desynchronisation. A baseline segment, shown within the highlighted box at -4 seconds is used to determine the relative change in power of the mu frequency band (8-12 Hz). A substantial decrease in mu band power can be observed, with gradual resynchronisation beginning 2.5 seconds after the trigger. (Pfurtscheller & Neuper, 1997)

From He et al (2015), motor imagery is considered an internal stimulus, rather than external like P300 or SSVEP. One disadvantage of using an internal stimulus is that brain modulation requires conscious effort from the subject, which can mean that controlling a brain-computer interface would require extensive training. The advantage of using an internal stimulus is that no supplementary devices are required to elicit specific responses, the subject elicits them voluntarily, giving users greater control and independence. Motor imagery paradigms have seen considerable usage, but are less popular than P300 or SSVEP due to the training requirements necessary for effective control. Zhang et al (2019) demonstrated using a linear support vector machine to classify a binary motor imagery task. It was determined that mean accuracy across datasets was between 83 and 85 percent. Aldea and Fira (2014) used linear discriminant analysis for binary classification of imagined left- and right-hand movement, demonstrating a performance that varied significantly between subjects (68-91%). Bhattacharayya et al (2011) used a variety of different classifiers, such as linear discriminant analysis and support vector machines, on a left/right hand imagery task. From the studies examined, motor imagery appears compatible with a wide variety of different classifiers. While the training time for using a motor imagery paradigm poses a dilemma for BCI uptake, the use of imagined movement allows for many different control signals for a brain-computer interface and allows for particularly intuitive control for advanced BCI such as in limb prostheses.

Classification

Support Vector Machines

One potential classifier algorithm that could be used in motor imagery brain-computer interfacing is the support vector machine (SVM). Noble (2006) defines a support vector machine as an algorithm that is designed to find the hyperplane that results in maximal separation of classes in feature space. For two dimensions this is simple to visualise as the line that best separates both classes, this principle being extended into hyperspace. Support vector machines typically work with linearly separable data, although can be augmented for nonlinear problems through the use of a 'kernel'. Support vector machines have also seen considerable use in brain-computer interfacing. Sharma et al (2022) used both support vector machines and a multilayer perceptron in a motor imagery classification task. Average performance for the support vector machine was 74.12 percent, indicating the suitability of SVM in motor imagery tasks. Likewise, in Bhattacharayya et al (2011), support vector machines were used in conjunction with linear and quadratic discriminant analysis for left/right hand motor imagery classification. Using a kernelized support vector machine, the highest accuracy achieved was 82.14%, outperforming LDA by 3 percent. Zhang et al (2019) utilised support vector machines in conjunction with sparse group spatial pattern feature extraction for a simple motor imagery task. It was reported that mean classifier accuracy for each participant ranged from 83.3 to 88.5 percent. From Bhattacharayya et al, it follows that support vector machines may be slightly better suited in motor imagery classifications.

Artificial Neural Networks

The other classification algorithm that was examined was the artificial neural network. An artificial neural network refers to a genre of classification algorithms designed off the brain. An artificial neural network is formed from one or often many layers of interconnected nodes which are designed to separate classes. Unlike support vector machines, neural networks natively function for both linearly and nonlinearly separable functions since the activation functions used for each node are also nonlinear. One specific type of neural network, highlighted by O'Shea and Nash (2015), is the convolutional neural network. A convolutional neural network includes layers of neurons that perform convolutions on clusters of their inputs. By clustering areas together in a convolution, the number of weights associated with the data is considerably decreased, which can allow for substantial decreases in computational complexity. O'Shea and Nash highlight mention that convolutional neural networks see particular use in image and pattern recognition, as the use of clusters can allow for the detection of larger features. Neural networks have seen significantly less use in motor imagery and brain-computer interfacing in general, although recent developments in deep learning have resulted in considerable interest in the area. Wang et al (2020) used convolutional neural networks for two and four-class motor imagery classification tasks. For the binary classification task, mean model accuracy was measured as 82.4 percent, decreasing to 65% for four-class classification. Similarly, Dose et al (2018) used a deep learning CNN for two and four class classification tasks. After performing a 5-fold cross validation, the mean performance for a cross participant classifier was 80.38 percent, correlating closely with the results found by Wang et al. Moreover, the results found by Dose et al were from a large participant dataset (n=109) indicating that the performance is unlikely to be anomalous. A recent study by Zhao et al (2022) used convolutional neural networks to classify participant data in a four-task motor imagery test. Average testing accuracy was measured as 72.13 percent, indicating success, although it was noted that there was limited cross-compatibility between subjects. It was recommended that a basic model could be pre-trained and then adapted according to the user, compromising between performance and training time. Comparing between support vector machines and neural networks, Sharma et al (2022) recently used both algorithms in to classify left and right hand, as well as right foot imagined movement. It was noted that the support vector machine got an average subject accuracy of 73.17 percent. By comparison, the neural network used; a multilayer perceptron, achieved a performance accuracy of 92.5 percent, indicating significantly better performance compared to the SVM. It should be noted that the number of subjects used for this study was low (n=4), meaning that additional testing may be required to confirm the validity of these results. It was also noted that the receiver operating characteristic curve was better far better for the multilayer perceptron, indicating that the network was better generalised and as such should be more applicable to previously unseen data. One potential disadvantage for neural networks is the computational complexity of the model, which can quickly grow depending on the complexity of the input data. With careful optimisation of the features used or network reduction

through the use of a convolutional neural network, it is possible to overcome this weakness without significantly impeding performance.

Gap Statement

While the potential of brain computer interfacing is exciting, with a significant body of literature written describing the various implementations of the technology, attempts to produce a commercially viable product have yet to be successful. Motor imagery paradigms offer the potential for intuitive control over more complex BCI though they are presently held back by high BCI illiteracy rates (Qiu *et al.* 2017 | Zhang *et al.* 2021). It has been suggested by Jeunet *et al.* (2016) that the reason for higher reported BCI illiteracy may be a result of poorly designed training protocols. To that end, a new methodology was proposed by Ostendorf (2022) which used a modified motor imagery paradigm which also included real movement. As real movements are easy to perform, it was hypothesised that combining real and imagined movements in a protocol would provide greater familiarity with the movements for imagining, improving training outcomes. Many studies that focus on developing BCI utilise EEG setups with many electrodes (Bian *et al.* 2018). While feasible in clinical settings, using 64-channel EEG is too time-consuming to setup for ordinary use and limits device portability. Simultaneously, the Laplacian technique for noise-filtering typically requires 64+ channel EEG setups, and can be computationally intensive, particularly when performed in real-time. To that end, it was hypothesised that tCRE could be used to bridge this gap. As such, this project aims to extend the previously proposed motor imagery method by Ostendorf (2022) to include the use of tCRE, reducing noise and improving classifier performance in a single electrode setup.

METHODOLOGY

Experimental Design

Participants

Data collection was conducted between May 18th and August 25th within the Multi Modal Recording Facility (MMRF) Faraday cage at Tonsley. Participants were volunteers recruited within the research group with no prior history of neurodegenerative disease or other health conditions which may have impacted performance.

Participant ages ranged from 22 to 49 (mean 33.5 ± 16 , $n = 7$) with five males and two females. One participant was left-hand dominant, while the remaining seven were right-hand dominant. Two members had previous experience with both EEG recording and the motor imagery paradigm specifically, while the remaining five members had no prior experience with EEG.

EEG Electrode Configuration

The EEG recording was performed using a CREmedical t-interface 20 (figure 3), connected with a g.tec 64-channel electrode connector box. The connector box then interfaced with a g.tec g.HIAMP multichannel amplifier, which transmitted EEG information to a recording script, written in python. The setup was composed of 27 channels; 13 tCRE, 13 emulated EEG and a single disc electrode was required for use as a reference. While tCRE electrodes have in-built references, a dedicated reference electrode was required for the multichannel amplifier to function correctly. It should also be noted that tCRE electrodes can also output emulated EEG signals using the outer ring of the electrode and as such only 14 physical electrodes were required in the EEG setup. TD-246-4 skin conductance electrode paste was used for the tCRE electrodes.



Figure 3 The CREmedical t-interface 20. 13 tCRE electrodes were connected from the participant into this interface, which interfaced with g.tec 64-channel connector box. Each tCRE electrode produced two outputs; an emulated EEG output generated from the outer electrode ring, and a tCRE output.

The tCRE electrodes were placed on an EEG cap with connection holes in accordance with the 10/5 system (figure 4), a higher density extension of the more traditional 10/20 system. Prior to placement of the EEG cap on the participant, an alcohol solution was used to scrub the participant's scalp, reducing impedance prior to the application of conductive gel. Midline markers were drawn on the participant's head by finding half the distance between each tragus, and between the inion and nasion. With midline markers drawn, the intersection between these lines represented the centre of the head and aligned with the location of Cz, seen in figure 4.

Once complete, the EEG cap was aligned with the centre point and secured tightly to the participants head to minimise movement. A single disc electrode was placed on the EEG cap as a reference, before applying Abralyt (Neurospec, Switzerland) conductive gel. It should be noted that tCRE electrodes have an intrinsic reference and as such do not require a reference electrode. However, for the amplifier to function correctly, a reference electrode must be included regardless. For consistency with the previous study (Ostendorf, 2022), the reference electrode was placed at Fz, located equidistant between hemispheres. Three tCRE electrodes were placed along the midline at Fpz, POz and Oz for use in preliminary diagnostics. Prior to commencement of the experiment, participants were asked to perform a series of tasks, such as eyes blinking or closed eyes relaxation. By examining the presence of heightened alpha band (8-12 Hz) activity in these diagnostic electrodes, the correct placement of the EEG cap was confirmed. Finally, ten electrodes were placed

over the left (FCC5h, FCC3h, C3, CCP5h & CCP3h) and right (FCC4h, FCC6h, C4, CCP4h, CCP6h) hemispheres of the sensorimotor cortex. These electrodes were to be used to detect event related desynchronisation occurring during any of the movements performed.

Figure removed due to copyright restriction.

Figure 4 EEG montage of the experimental setup in accordance with the 10/5 system. The black electrode locations are derived from the standard 10/20 system, with grey and white electrode locations derived from the 10/10 and 10/5 systems, respectively. The location circled with purple (Fz) correlates with the position of the reference, while the midline electrodes marked with blue were used in preliminary diagnostics. The electrodes marked with green were located over the sensorimotor cortex and were used for observing ERD during the experiment. (Ostendorf, 2022)

EMG Electrode Configuration

Three electrodes were adhered to the participant's right forearm, correlating with the arm involved in the target movements of the experimental protocol. Two electrodes were placed over the extensor digitorum, responsible for extension of the four medial digits and the primary muscle involved in the target movements. The tertiary electrode was used as a ground and was located distally on the forearm.

Experimental Protocol

Motor Imagery Paradigm

The experimental protocol used was a form of motor imagery paradigm that incorporated real and imagined movements to trigger an event related desynchronisation. As part of the experimental protocol, three separate hand movements were to be performed using the participant's right hand. Between movements, the participant was asked to keep their right forearm pronated on the desk with their hand in a relaxed but enclosed fist. By resting the participant's arm on the desk, it was hoped that this would reduce unnecessary movements of the arm, minimising potential muscle artefacts and decreasing fatigue during the protocol. The 'half stretch' movement involved the participant unfurling their fingers from a fist, without total extension. The 'full stretch' movement involved the participant fully extending their fingers. The 'imagined' movement involved the participant keeping their hand in a resting position and imagining full extension of the fingers.

Participants were situated in front of a computer which displayed a series of prompts to guide them through the protocol. Prior to initiation of the protocol, an introduction was displayed on screen, telling the participant to minimise unnecessary movements during each instruction segment, as well as explain the three target movements. Prompts were displayed visually on-screen as well as delivered verbally. After introducing the target movements, a period was given for the participant to practice each of the movements until they felt comfortable. Participants were given a prompt to continue with the experiment, once they felt sufficiently prepared with the target movements.

Figure removed due to copyright restriction.

Figure 5 Target movements performed as part of the experimental protocol. Participants were given a video prompt to perform one of the three movements, accompanied with a bell sound to signify when movement should occur. Half and full stretch movements involved extension of the fingers by contraction of the extensor digitorum in the forearm, with half and full movements distinguished by the amount of extension performed. Imagined movement involved imagining full extension of the fingers without any physical movement (Ostendorf, 2022).

Once the participant was ready, the recording phase commenced, consisting of 60 movements, divided equally between half, full and imagined stretches. The 60 movements were subdivided into 6 groups of 10, with resting periods dispersed in-between. By providing adequate resting opportunities between each movement block, it was hoped that this would reduce mental and physical fatigue in the participant, as well as allow opportunities for free movement to reduce

fidgiting during the recording periods. The target movement prompts were ordered randomly throughout the protocol, to minimise participants anticipating movements. Each prompt was displayed on-screen for a period of 5 seconds, accompanied with a bell sound to signify when the participant should perform the movement. Each prompt was faded onto the screen over a period of 0.8 seconds. By including a fading transition, it was hoped that any P300 response to the stimulus could be avoided. An interval of 2 seconds was included between prompts to ensure there was sufficient time for the sensorimotor cortex to return to baseline after an event related desynchronisation.

Figure removed due to copyright restriction.

Figure 6 Layout of each video prompt. From 0 to 0.8 seconds, a fade in transition was used to avoid triggering a visual P300. From 1.3 to 3.3 seconds, a soft bell sound was played to signify when participants should conduct the designated movement, with a fade-out transition also included from 4.3 to 5 seconds. Event markers were distributed at each of the marked times for use in the processing phase. (Ostendorf, 2022)

Event markers were distributed at the beginning and end of each transition, as well as either side of the sound playing, in order to simplify tracking EEG activity in regard to the target movements. Additionally, the type of movement performed (half, full & imagined) was marked, to simplify sorting the movements during processing.

EEG Signal Processing

Processing of the collected EEG data was performed in MATLAB utilising the EEG3, Signal Processing and Statistical & Machine Learning toolboxes. Using the event markers included during the recording phase, the EEG recording could be subdivided into a series of epochs for use in visualising ERD, as well as in classifier training. To establish a baseline to determine if an event related desynchronisation occurred, one second of data was taken from before the start marker. To process the EEG data, a method put forward by Pfurtscheller & Lopes da Silva (1999) was used involving:

- Bandpass filtering the target frequency band (8-12 Hz)
- Squaring of amplitude samples to obtain power samples
- Epoching participant data, separating by electrode and target movement

Using the baseline segment prior to each start marker, from -1 to 0 seconds, a reference value was determined for calculating the relative ERD observed during the movement. From Pfurtscheller & Lopes da Silva (1999), the relative ERD was calculated for each epoch by using equation 1, where the variable A is substituted with the recorded power.

Equation 1 Converts the ERD to a percentage change in mu power amplitude, based on a baseline reference, R , extracted from -1 to 0 seconds.

$$ERD(\%) = \frac{A - R}{R} \times 100$$

EMG Signal Processing

The EMG data was processed using a similar method (Pfurtscheller & Lopes da Silva, 1999), for use in observing muscle activity during the movements performed:

- Bandpass filtering the target frequency band (8-12 Hz)
- Squaring of amplitude samples to obtain power samples
- Epoching participant data, separating by electrode and target movement

The EMG data was collected to observe the expected differences in muscle activity during half, full and imagined movements. As the imagined movement required the participant to keep their hand relaxed, the EMG was of particular interest to confirming that these instructions were complied with.

Classification

Electrode Selection

In brain computer interfaces, it is desirable for the sensory modality used to be simple and unintrusive. It is not feasible for users to wear a full EEG setup constantly, as it would be difficult and time consuming to set up and the inclusion of additional wires may limit movement and manoeuvrability even further. To simulate use in a BCI, a single electrode was picked for each participant, based on the electrode displaying the greatest difference in mu rhythm power between synchronised and desynchronised states. A script was created in MATLAB (see appendix A) to calculate the difference in mean time amplitude between the baseline segment from -1 to 0 seconds, and the movement segment, from 0 to 5 seconds. The reported best-performing electrode for each participant was collected for both emulated EEG and tCRE, seen in table 1.

Table 1 Electrodes demonstrating the greatest change in mu band power during an event related desynchronisation, ordered by participant and sensory modality used.

Participant	1	2	3	4	5	6	7
Emulated EEG	CCP6h	CCP5h	FCC5h	CCP4h	FCC5h	FCC4h	CCP5h
tCRE EEG	CCP6h	FCC5h	FCC5h	CCP6h	FCC5h	CCP6h	FCC4h

Support Vector Machine

To allow for comparison with results collected during the previous project (Ostendorf, 2022), and to answer RQ2: *What differences can be observed in event related desynchronisation between tCRE and emulated EEG?* a support vector machine was trained from the collected EEG data. As part of this method, the feature space of the data used was reduced by resampling epochs at 300 Hz, rather than 1200 Hz, sufficiently high to avoid aliasing while decreasing the complexity of the support vector machine substantially. For comparison with Ostendorf (2022), the dataset used for training and testing the support vector machine was derived by subdividing each epoch into 3 training samples. A 1-second sample was collected from before and after each movement block (-1 to 0s & 5 to 6s, respectively) correlating with synchronised mu activity and defined as 'class 1'. The remaining sample was collected from the middle of the event block (2 to 3s), correlating with desynchronised mu activity, and defined as 'class 2'. As such, given 3 samples were collected per epoch, with 60 epochs collected per participant, a dataset consisting of 540 samples was created for each participant.

Figure removed due to copyright restriction.

Figure 7 Annotated layout of each video prompt for generation of training samples. The regions marked in blue (-1s to 0s & 5s to 6s) were extracted from either side of the video prompt and correlated with synchronised mu activity, labelled as 'class 1'. The region marked in green (2s to 3s) was extracted from the middle of the video prompt, corresponding to mu desynchronisation and labelled as 'class 2'. (Ostendorf, 2022)

The support vector machine was trained using leave-one-sample-out (LOSO) cross-validation. Leave-one-sample-out is a variation of leave-one-subject-out, which is typically used for reducing subject bias in classifiers trained on multiple participant datasets. Using LOSO cross-validation, a single sample is used for testing, while the remaining samples are used during testing. This process is repeated, cycling through every sample to determine the performance of the classifier. Note that each classifier was trained on a dataset from a single participant, rather than from all participants.

While the general mechanisms for event related desynchronisation are the same in all people, the signals themselves are highly individualistic. While generalisation is beneficial in that the BCI could be used by more people, BCI is an assistive technology designed to suit the individual. As such it would be better to train the classifier on an individual specifically, capturing idiosyncratic characteristics and ensuring better performance.

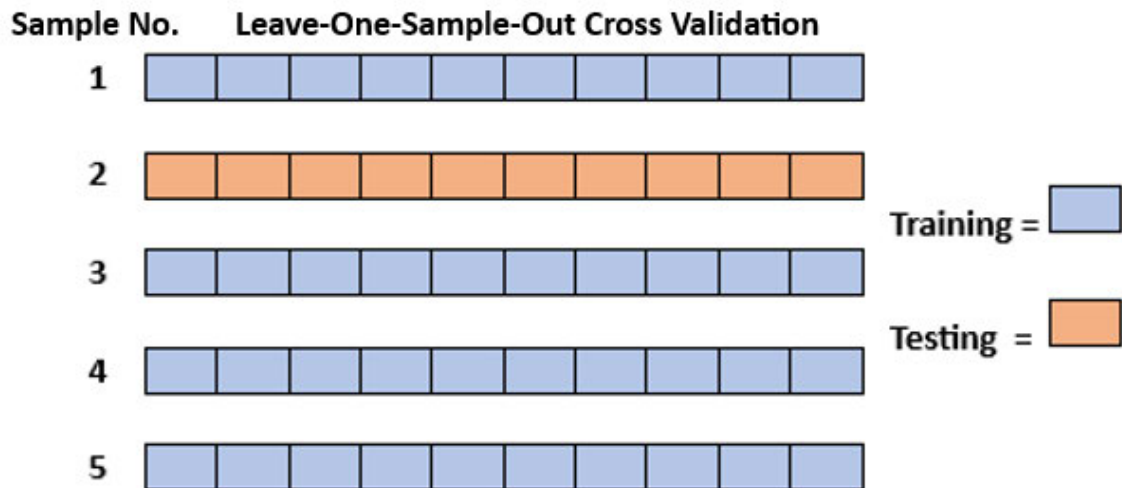


Figure 8 Leave-one-sample-out cross validation. In LOSO cross-validation, a single sample is reserved for use as the testing dataset, while the remaining samples are used for training the classifier. To determine overall classifier performance, this process is repeated, such that every sample has been isolated for use in testing.

Neural Network

Extending from previous work and to answer *RQ4: What differences in training performance can be observed between support vector machine and neural network algorithms?* a neural network was also trained using collected EEG data. To increase the size of the training set, as well as improve classifier adaptability, the entire epoch was subdivided into 0.5 second training segments. Segments located outside of the movement markers (<0s & >5s) were marked as synchronised mu and assigned to class 1, while segments located between were marked as desynchronised mu and were assigned to class 2. The meantime power of each segment was calculated and stored for use in training the neural network. Various network sizes were used, with the results displayed using a smaller network topology that included two hidden layers with four nodes each. By using a smaller network, it was hoped that training times could be kept low, while achieving acceptable performance. To avoid biasing the neural network towards either class, a script was created to measure differences in the size of the two classes and randomly remove samples such that both classes had the same number of samples included (see appendix B).

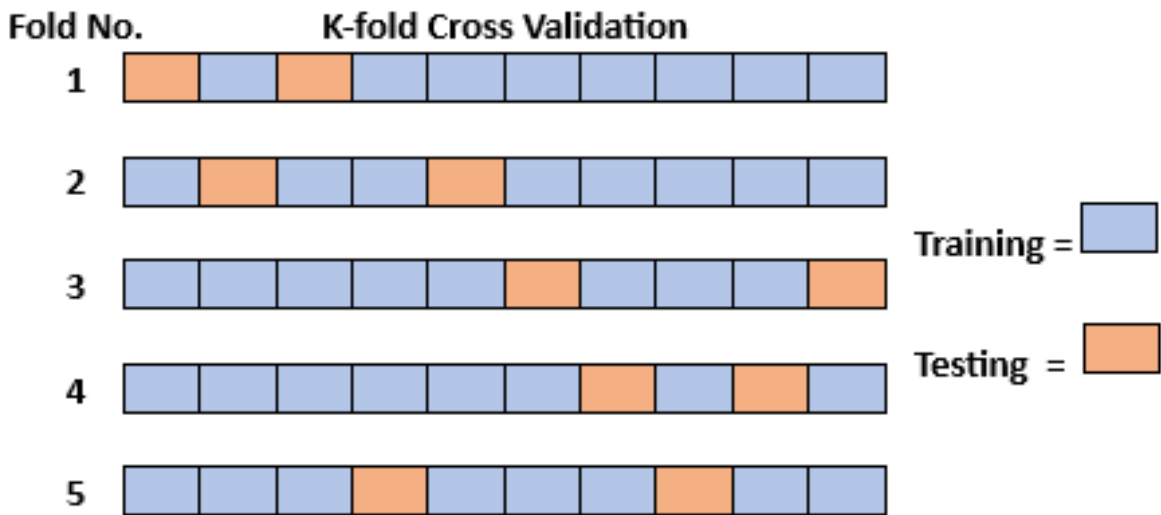


Figure 9 K-fold cross validation. In K-fold cross validation, a dataset is subdivided into K folds, with K-1 folds used as a training set for the classifier. The remaining fold is then used during testing. This process is repeated such that all folds have been used in both training and testing phases.

The neural network was trained using K-fold cross validation. In K-fold cross validation, the dataset is subdivided into K sets of data, with one set reserved as testing data, and the remaining being used during training. The process of training and testing is then repeated K times such that every fold has been used as testing, with the performance determined by finding the mean and standard deviation between folds.

RESULTS

Event Related Desynchronisation

Emulated EEG

To answer RQ2: *What differences can be observed in event related desynchronisation between tCRE and emulated EEG?*, the event related desynchronisation was plotted, relative to an initial baseline defined from -1 to 0 seconds. Examining the processed EEG data from participant 1, seen in figure 10, a noticeable decrease in relative power within the mu frequency band could be observed across all movements from 1 to 4 seconds before gradual resynchronisation, indicating successful demonstration of ERD. Note that the vertical lines in each graph correlate with the timings of the event markers. Black markers signify the beginning and end of the video, blue lines indicate the timing on the fading transition, and the red lines signify when the bell sound was played.

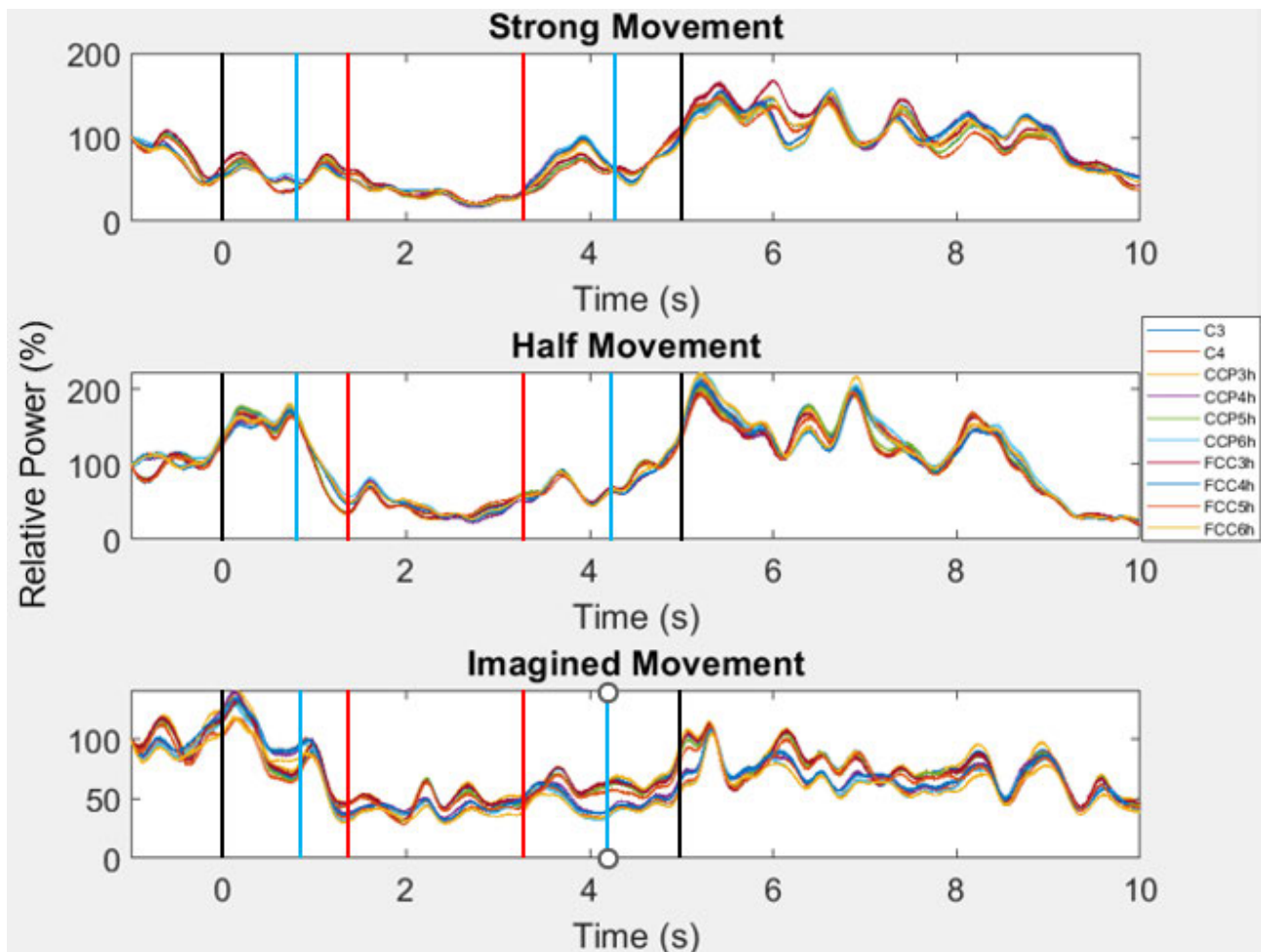


Figure 10 Mu frequency band activity for participant 1, separated by electrode and movement. Mu power was measured as a percentage change, relative to an initial baseline generated from -1 to 0 seconds. Across all electrodes and movements, an event related desynchronisation could be observed, marked by the substantial decrease in mu band power from 1 to 4 seconds. It was noted that there was little mu resynchronisation present in the imagined movement, compared with both strong and half movements.

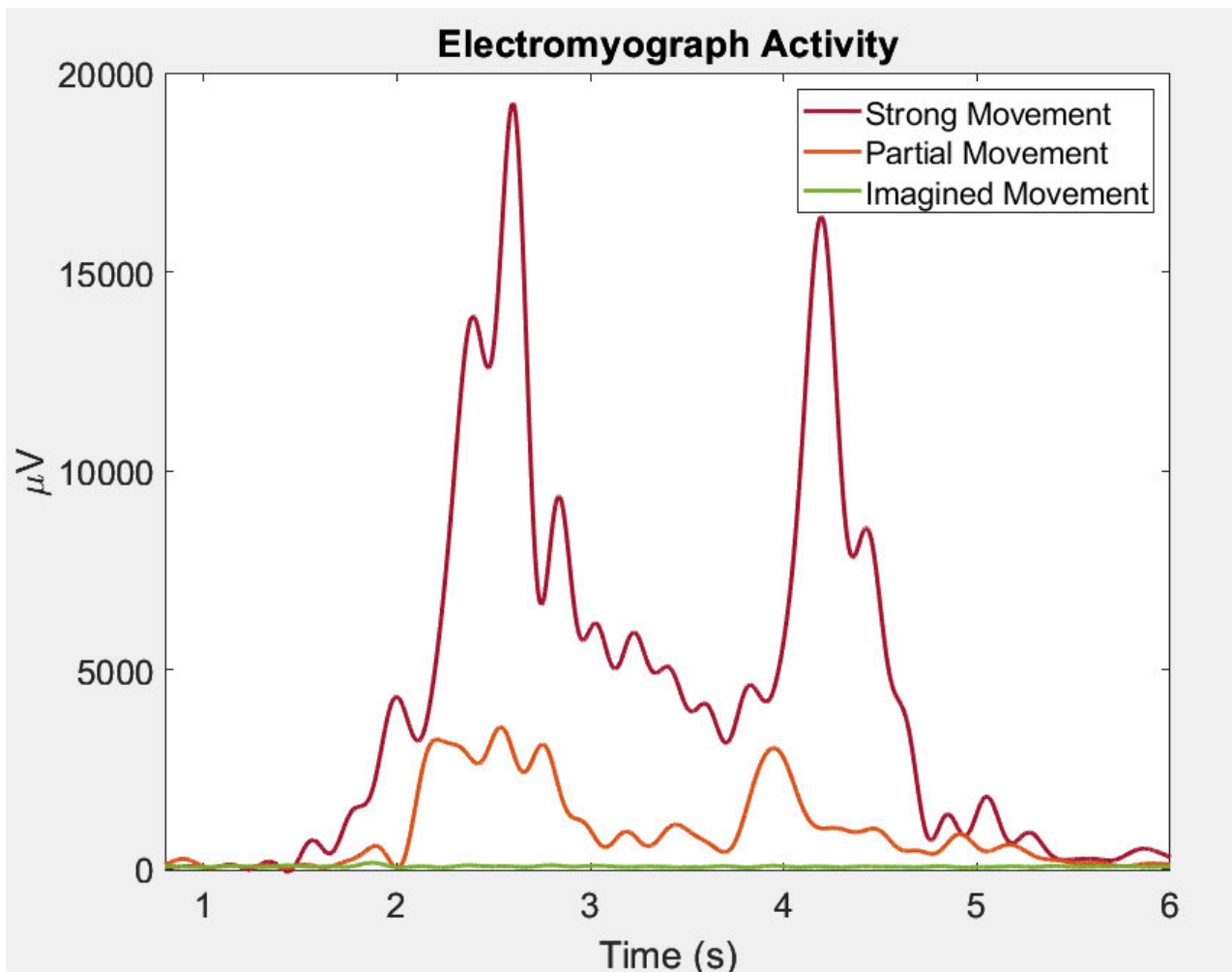


Figure 11 Electromyograph activity of participant 1, averaged across epochs and separated by movement. As expected, strong movements involving maximal extension of the extensor digitorum produced a substantially larger EMG response, compared to the other movements. Two peaks were noted in the EMG, likely correlating to extension and then flexion of the fingers. Partial movements, displayed in orange exhibited these same two peaks in EMG activity, with reduced amplitude compared with strong movements. Imagined movements produced negligible EMG activity, indicating that participant 1 maintained relaxation while imagining full extension of the fingers.

Examining figure 11, the recorded electromyograph activity for participant 1 can be observed across each of the target movements. As expected, strong movements demonstrated the highest amplitude increase during movement, with dual peaks at the beginning and end of the movement. Similarly, partial movement also demonstrated elevated EMG activity, albeit to a reduced degree. Importantly, EMG activity was substantially reduced from both half and full movements, with no dual peak observable. As such, it was likely that the EMG present was mostly external noise or artefacts from other muscles, rather than movement of the forearm, specifically.

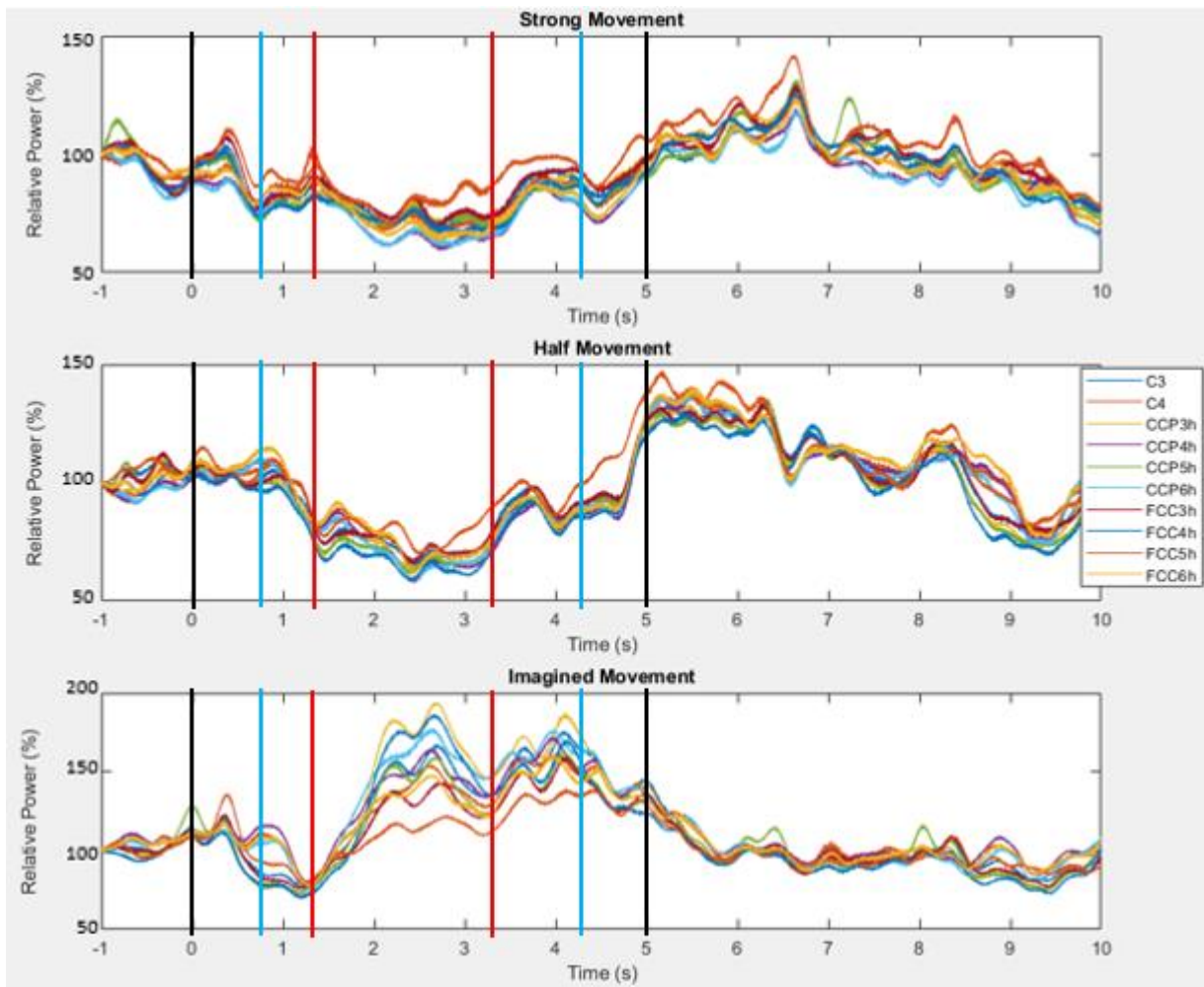


Figure 12 Emulated EEG Group average relative mu band power, separated by electrode and movement. Strong movement demonstrated a slow decrease in mu power, with an approximate 40% decrease over 3 seconds, before resynchronising. Half movement demonstrated a sharper decrease in mu power over 2 seconds, before substantial resynchronisation above the baseline. Most notably, imagined movement appeared to demonstrate an increase in mu band power of almost 100%.

Examining figure 12; the emulated EEG group average, event related desynchronisation can be observed across all electrodes, averaged across participants. As expected, a decrease in relative mu band power can be observed in the strong and half movements, indicating the presence of ERD. Interestingly, the group average imagined movement response demonstrated an increase in relative mu band power, deviating from the real movements.

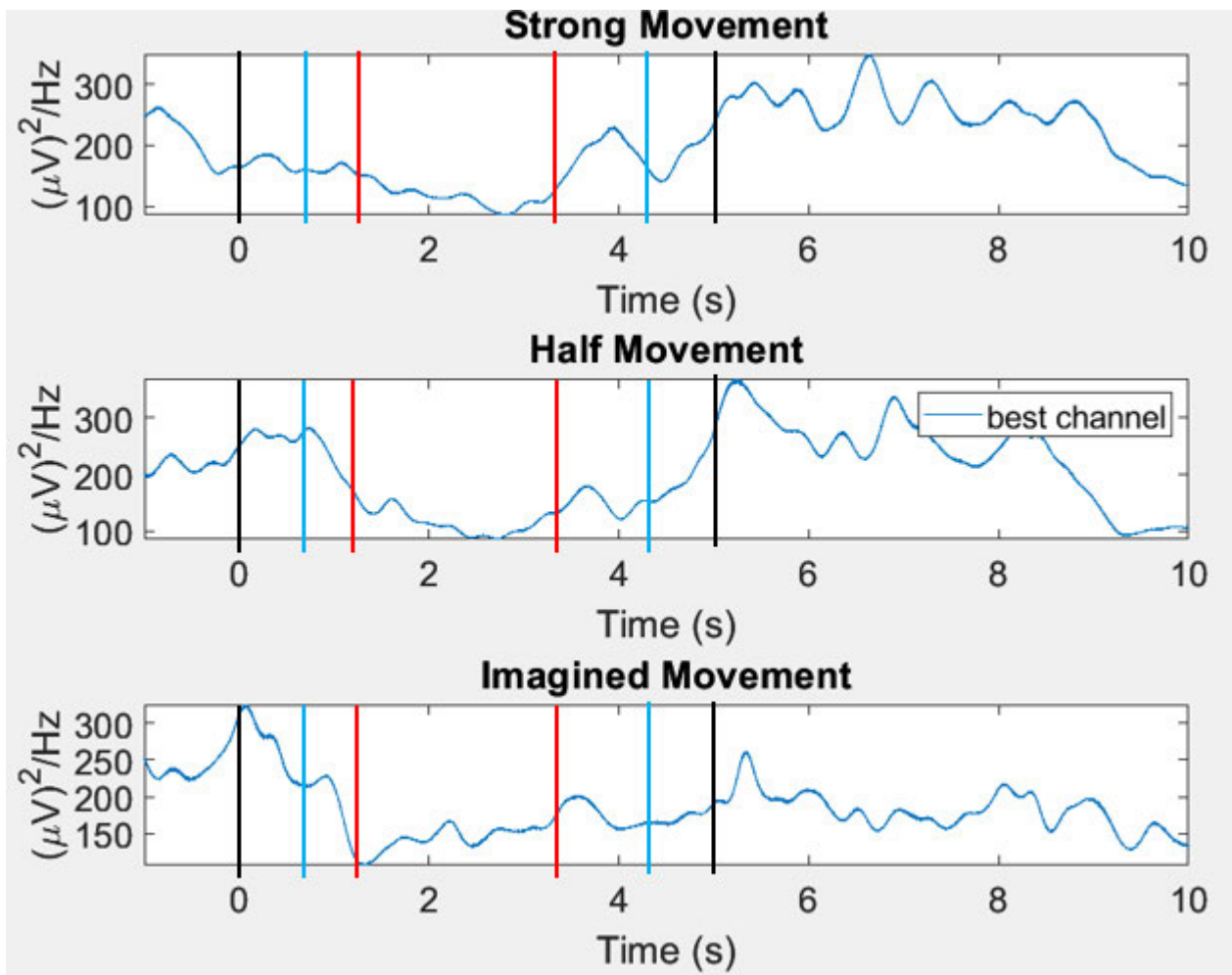


Figure 13 Absolute ERD group average using corresponding best channel. Best channels were determined for each participant by finding the electrode recording the greatest desynchronisation. Across all movements, a desynchronisation of 50-60% was observed. Both strong and half movements demonstrated a noticeable resynchronisation from 4 to 6 seconds. Imagined movement had little resynchronisation occur after movement completion.

Averaging the best performing channel across participants, figure 13 shows the resulting response. Across all movements, event related desynchronisation could be observed, occurring between 0 and 1.8 seconds. Both strong and half movements demonstrate an obvious resynchronisation of relative mu power from 4 seconds. In contrast, imagined movements had little obvious resynchronisation occurring even up to 10 seconds.

tCRE EEG

To answer RQ1: *Can event related desynchronisation be observed using tripolar concentric ring electrodes?*, the event related desynchronisation of participant 1 was again plotted, instead using tCRE. Examining figure 14, the presence of ERD is substantially less obvious, with limited similarities between electrodes.

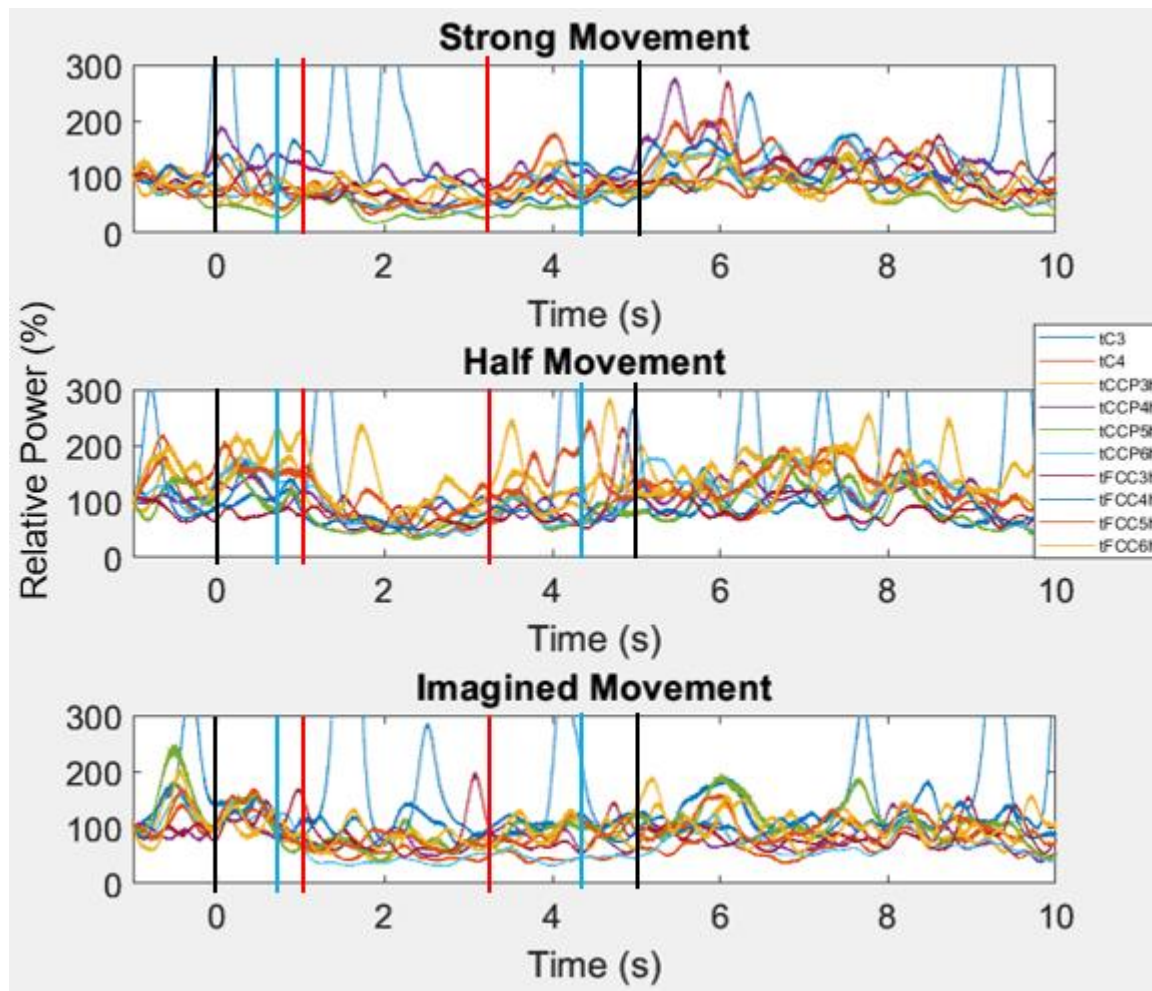


Figure 14 Participant 1 mu band power using tCRE, separated by electrode and movement. Electrode activity appeared more chaotic, suggesting reduced cohesion between electrodes. The presence of event related desynchronisation isn't obvious, likely present only in electrodes close to the region of activation.

From the group-average tCRE, a desynchronisation of 25-50% was observed across all movements from 2 to 4 seconds, seen in figure 15. Examining figure 15, it was noted that there was no surge in mu band power in the imagined movement, indicating not only that the outlier was a result of a muscle artefact, but also that the tCRE was capable of attenuating this artefact. This supports the claim that tCRE is better at attenuating distant noise sources.

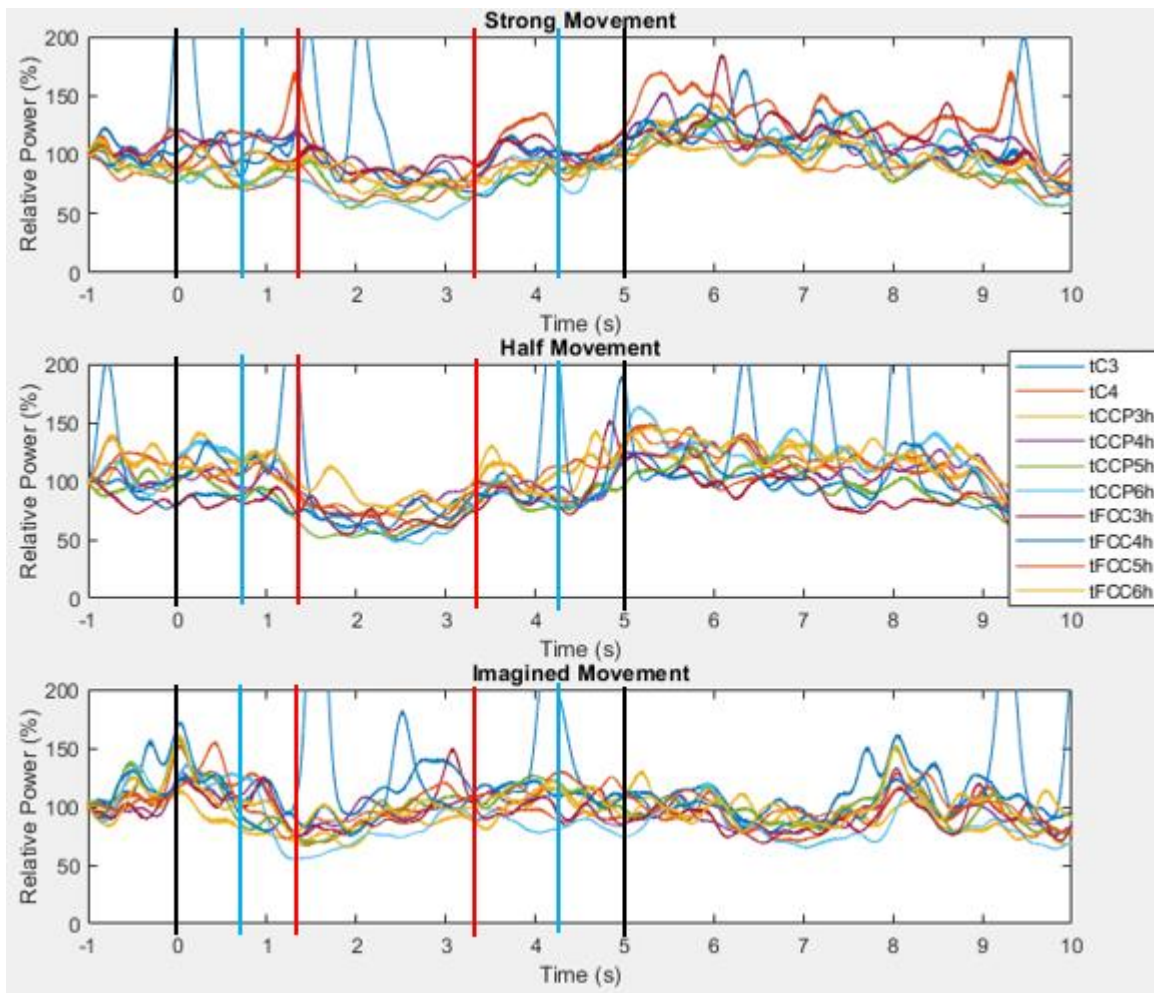


Figure 15 Group average relative mu band power, separated by electrode and movement. Strong movement demonstrated a slow decrease in mu power, with an approximate 30% decrease over 4 seconds, before resynchronising. Half movement demonstrated a similar decrease in mu power over 2 seconds, before resynchronisation back to baseline. Imagined movement demonstrated sharp desynchronisation, before gradually resynchronising over 3 seconds. Interestingly, there was no outlier in the imagined movement as in the emulated EEG data, suggesting that tCRE successfully attenuated the disturbance that caused it.

Averaging the best performing electrode across participants, the group average response for each movement was determined. From figure 16, event related desynchronisation could be observed across all movements, indicating success with detecting ERD using tCRE. Both strong and half movements demonstrate resynchronisation of mu band power from 5 seconds, while imagined movement shows little resynchronisation occurring.

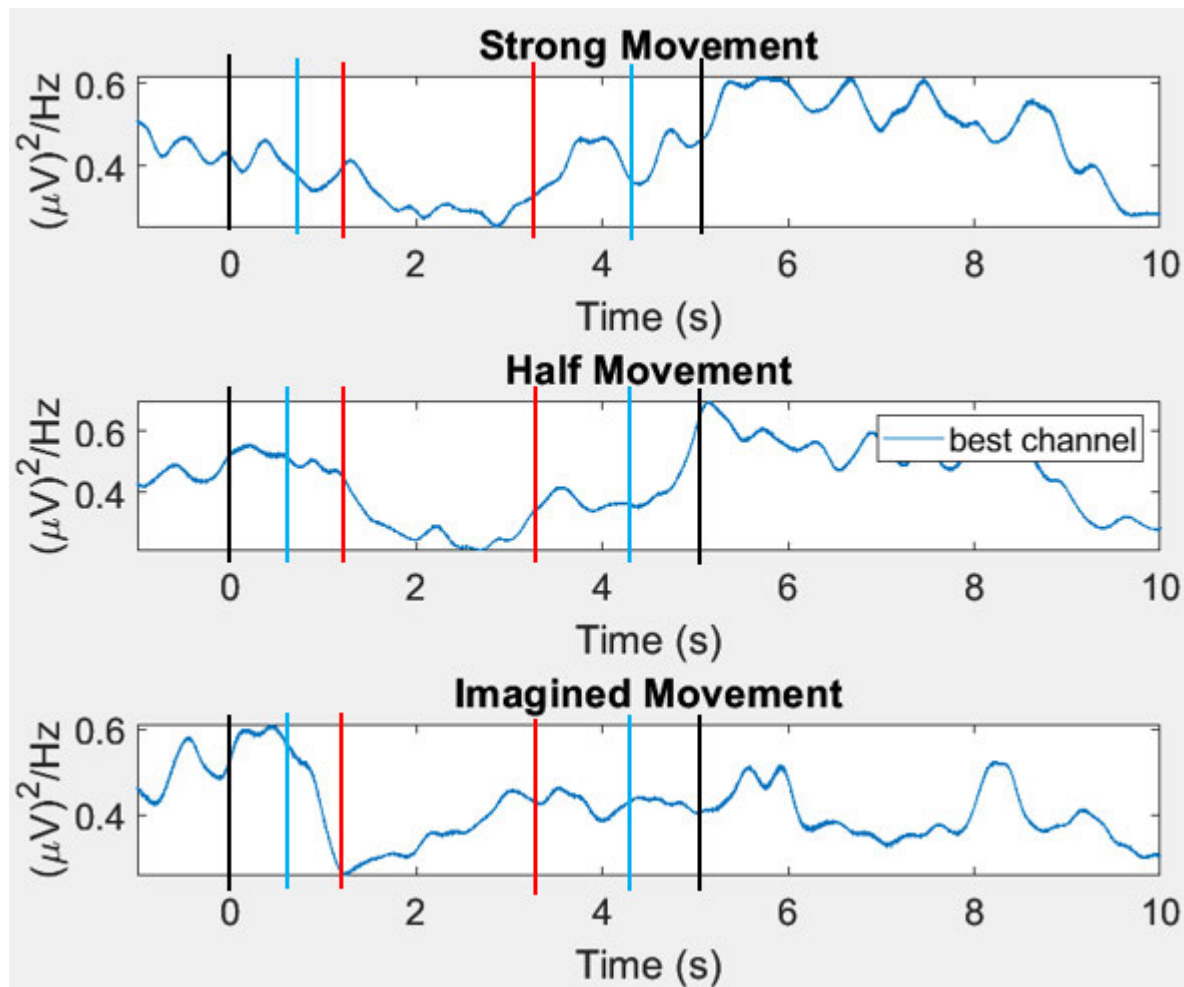


Figure 16 tCRE absolute ERD group average using corresponding best channel. Best channels were determined for each participant by finding the electrode recording the greatest desynchronisation. Across all movements, a desynchronisation of approximately 50% was observed. Both strong and half movements demonstrated a noticeable resynchronisation from 4 to 6 seconds, exceeding baseline. Imagined movement appeared to resynchronise quickly, returning to baseline by 3 seconds.

Classification

Support Vector Machine

Classifiers were tested on participants individually using the best performing electrode. To answer RQ3: *How does training an ERD classifier on tCRE data influence accuracy, in comparison to ordinary and emulated EEG?*, a support vector machine was trained using tCRE and emulated EEG. To determine classifier performance, LOSO cross-validation was used on each participant, with the mean performance determined. A confusion matrix of the performance across participants using emulated EEG was created, seen in figure 17(left). From the confusion matrix, a mean accuracy of

66.8% \pm 3.71 was reported for emulated EEG, with each classifier demonstrating notable favourability towards class 1 (synchronised mu).

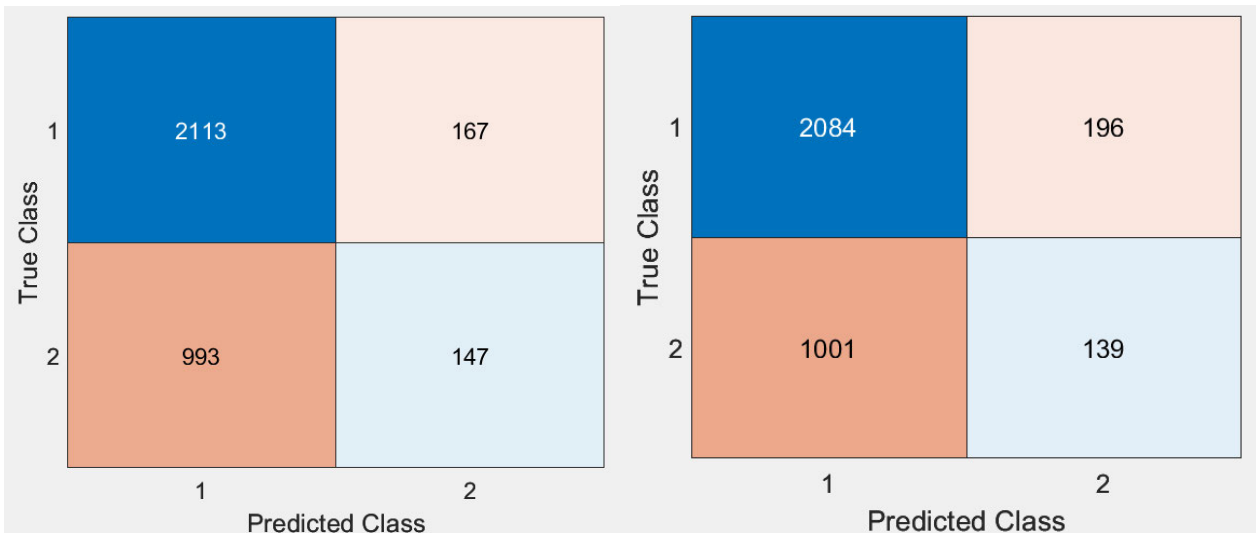


Figure 17 Support vector machine group average confusion matrices. Trained on the emulated EEG (left) and tCRE (right) datasets. A noticeable difference in the values of either half can be observed, with class 1 predictions accounting for 88%. This suggests very strong favourability towards class 1 (synchronised mu activity).

Similarly, a support vector machine was also trained using participant tCRE data, with a group confusion matrix displayed in figure 17(right). Using tCRE, the support vector machine achieved a mean accuracy of 65.6% \pm 1.69, comparable to emulated EEG performance. Examining figure 17(right), it was again noted that there was clear favourability towards class 1 (synchronised mu), indicating the potential presence of class bias.

Neural Network

To answer RQ4: *What differences in training performance can be observed between support vector machine and neural network algorithms?*, a neural network classifier was trained, to compare its reported performance with that of the tested SVM. Each neural network was trained on data collected from a single participant, first on emulated EEG, then on tCRE. A confusion matrix was generated of the neural network's performance, seen in figure 18(right). The neural network achieved an accuracy of 58% using emulated EEG, notably lower than with the support vector machine. Analysis of the confusion matrix in figure 18(right) also shows slight favourability towards synchronised mu activity (class 1). Extending across all participants, the accuracy of the neural network was calculated as 51.7% \pm 1.01 for emulated EEG. It was noted that since each confusion matrix was generated over a single K-fold iteration, and hence didn't include averaging, the reported accuracy of the confusion matrix was higher than the actual performance of the network.

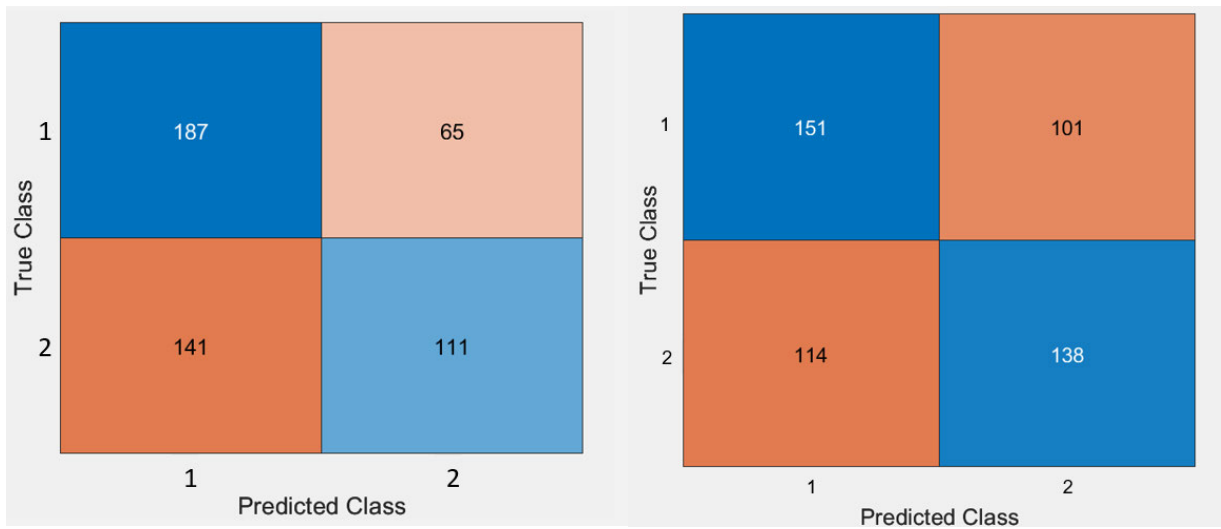


Figure 18 Neural network confusion matrices for participant 1, trained on the emulated EEG (right) and tCRE (left) datasets. Despite balancing the class distribution used during training, the emulated EEG classifier still demonstrated favourability towards predicting class 1 (65% of predictions). The tCRE classifier showed more balanced class prediction, with only 52% of predictions for class 1.

After analysing the emulated EEG dataset, the neural network was reconfigured to be trained from tCRE data instead. Examining figure 18(left), a confusion matrix was generated from participant 1, indicating an accuracy of 57%, comparable to the results achieved using the emulated EEG dataset. It was noted that the tCRE dataset appeared to lean less heavily towards class 1 predictions, with predictions distributed evenly on the confusion matrix. Extending across all participants, the neural network classifier achieved an accuracy of $52.7\% \pm 0.90$, indicating slightly higher accuracy, compared with emulated EEG.

DISCUSSION

Comparison With Literature

Experimental Protocol

As part of meeting *RO1: Using a motor imagery paradigm, collect EEG data with tCRE*, modifications were made to the protocol proposed by Ostendorf (2022) to utilise tripolar concentric ring electrodes. Burianova *et al* (2013) proposed a novel paradigm for implementing motor imagery in magnetoencephalography (MEG) and functional magnetic resonance imaging (fMRI). The paradigm involved the real and imagined flexion of the fingers, consisting of four blocks of four movements, separated by 21 second rest blocks. It was noted in this study that despite the inclusion of longer rest times between movement blocks, all participants reported greatly elevated fatigue, suggesting that fewer blocks may be beneficial in reducing fatigue. It was noted that Burianova *et al* (2013) included a 30-minute training session 48 hours prior to participation with the experiment, simulating 10 trial runs through the protocol and ensuring familiarity. Examining the recorded electromyograph activity between participants within this study, it was noted that two participants demonstrated elevated EMG during imagined movements, indicating potential BCI illiteracy and difficulty with the paradigm. The percentage of participants struggling with the motor imagery paradigm (approx. 30%) aligns with BCI illiteracy rates within the literature, with similar studies testing the motor imagery paradigm reporting between 10% and 50% of participants struggling (Qiu *et al.* 2017 | Zhang *et al.* 2021). By including more extensive training in the experimental protocol, as in Burianova *et al* (2013), it may be possible to subsequently improve familiarity with the movements and lead to an improved outcome. Alternatively, the inclusion of several follow-up sessions for participants using the same protocol may allow for increased practice, improving familiarity with the protocol, although it is unclear if this would significantly improve reported BCI illiteracy.

Event Related Desynchronisation

Examining the review of event related desynchronisation in EEG by Pfurtscheller and Lopes da Silva (1999), several examples of ERD could be used as comparison. As in figure 2, their figures presented event related desynchronisation initiating before their trigger, with a decrease of 50 to 100% within the relative amplitude of the mu frequency band during desynchronisation. Examining the response of participant 1, seen in figure 10, a 50 to 70% decrease in the mu frequency band was observed across all movements. While the change in amplitude was less than reported by Pfurtscheller and Lopes da Silva, it is indicative of event related desynchronisation occurring, partially fulfilling the requirements of *RO2: Identify the presence of event related desynchronisation within emulated EEG and tCRE EEG data*. Examining the group average response in figure 12, a decrease in amplitude of approximately 30% was observed, noticeably less than in figure 10, indicating that some participants may have demonstrated a reduced desynchronisation in association with the movements.

It was noted when examining the group average imagined movement response in figure 12 that there was an increase in mu band power, contrary to what was observed in participant 1, and within the literature itself. Comparing with Ostendorf (2022), a similar phenomenon was observed, occurring as an outlier during the recording phase. Examining each participant individually, it was noted that participant 6 recorded a 1200% increase in mu band amplitude from baseline, which could not be observed in other participants. An increase in amplitude of that magnitude was unlikely to occur from brain activity, indicating the potential presence of muscle artefacts. While participant 6 did demonstrate elevated EMG activity during the imagined movement segments, it was insufficient to explain the presence of elevated mu. It was theorised that this may have been the result of unintentional head movement during the imagined movement segment, causing a massive disturbance in reported mu rhythm power.

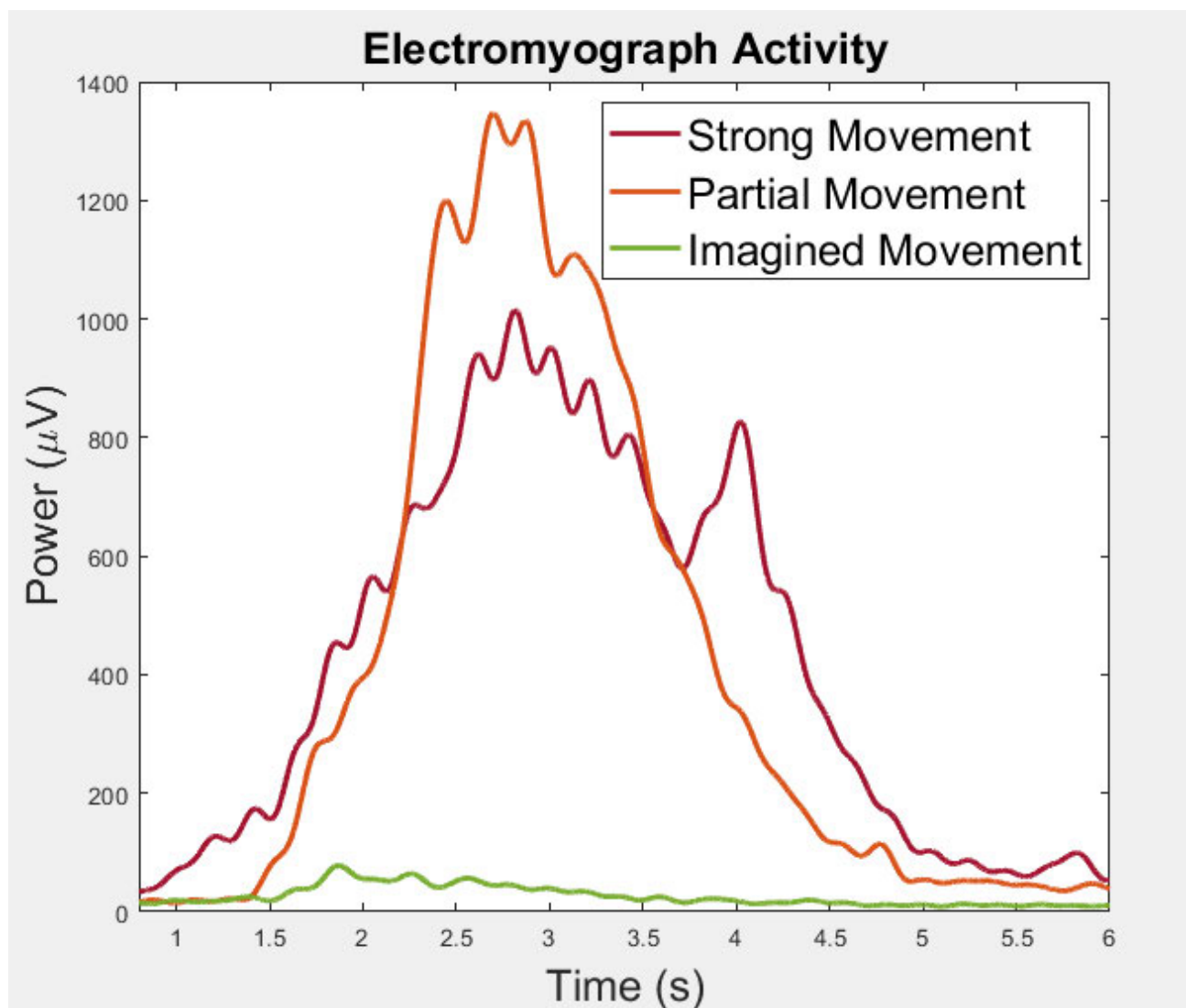


Figure 19 EMG activity of data outlier; participant 6. One discrepancy noted was that strong movement exhibited less power than the partial movement. Additionally, it was noted that EMG activity occurred during the imagined movements. The results indicate that the participant may have struggled or had poor understanding of the movements required.

To fully satisfy *RQ2: Identify the presence of event related desynchronisation within emulated EEG and tCRE EEG data*, the response of each participant using tCRE was also examined. Figure 14 correlates with the response of participant 1 across movements. Comparing directly with figure 10, it was noted that the data collected by tCRE appeared far more chaotic, indicating that signals were more distinct between electrodes. Literature has shown that EEG conducted with tCRE exhibits reduced mutual information between electrodes (Koka *et al.* 2007 | Liu *et al.* 2013). It was theorised that the noticeable differences in the activity of each electrode in the tCRE data was a result of this decreased mutual information, with desynchronisation more localised to specific electrodes closer to the activated region. To better visualise ERD, the electrode demonstrating the greatest change in mu band activity was used and averaged across participants, seen in figure 16. An approximate 30% decrease in mu band power was observed across all movements, aligning with the group average response using emulated EEG, and demonstrating that tCRE can be used to identify ERD. To answer *RQ2: What differences can be observed in event related desynchronisation between tCRE and emulated EEG?*, the decrease in mu band power during ERD is comparable between modalities. Although the literature around using tCRE for the detection of ERD is limited, one dissertation produced similar results, observing event related desynchronisation with reduced coherence between neighbouring electrodes (Alzahrani, 2019). Another study found that tCRE demonstrated improved cancellation of distant noise sources, with a similar level of performance identifying ERD between tCRE and emulated EEG (Tang, 2021).

Classifier Performance

To answer *RQ3: How does training an ERD classifier on tCRE data influence accuracy, in comparison to ordinary and emulated EEG?*, a support vector machine was trained on participant tCRE and emulated EEG data. A mean accuracy of 66% was achieved using emulated EEG, with a comparable mean accuracy of 65% achieved using tCRE. This would suggest that despite offering improved spatial selectivity, tCRE has no perceived advantage over emulated EEG in the training of support vector machine classifiers. One study that tested the effects of movement complexity on classification performance with support vector machines reported a mean accuracy of 84% for simple dynamic visual tasks (Bian *et al.* 2018). It was noticed that one distinction between methodologies was that they used a 64-channel EEG setup, selecting 35 channels for use in training their classifier. It is possible that a reason for the difference in reported accuracies could be attributed to this difference in channels used, with additional channels potentially providing more robust information for training the classifier. Furthermore, participants in Bian *et al.* (2018) performed 200 movements, compared to the 60 movements per participant in this study. It is highly likely that this also contributed to the difference in reported accuracies. To evaluate the credibility of this theory, the support vector machine was retrained, using all electrodes, rather than only the best performing electrode. Examining the new confusion matrix, seen in figure 20, a substantially higher accuracy of 88% was

observed, aligning more closely with the results put forward by Bian *et al* (2018), suggesting that the number of channels used has a large impact on classifier performance.



Figure 20 Confusion matrix of support vector machine performance on participant 1 using all electrodes. The reported accuracy for both emulated EEG (left) and tCRE (right) was 88%, substantially higher than with a single electrode and aligning more closely with the results found in the literature.

To answer RQ4: *What differences in training performance can be observed between support vector machine and neural network algorithms?*, a neural network classifier was also trained on emulated EEG and tCRE datasets. A mean accuracy of 51.7% was achieved using emulated EEG, while tCRE achieved a mean accuracy of 52.7%, substantially less than the observed performance of the support vector machine. A study by Sharma *et al* (2022) comparing support vector machine and neural network classifiers found opposing results, with the neural network demonstrating a slightly higher overall accuracy (82% versus 80%). It was noted that participants in that study were asked to perform 420 movements, providing a significantly larger training set. Additionally, more channels were used for training their classifier (35 versus 1), which likely contributed to their higher reported performance. Nicolas-Alonso *et al* (2012) does suggest that while neural networks can demonstrate better performance compared to support vector machines, their performance is more reliant on larger datasets, corroborating the deviation in reported accuracy with the literature. In hindsight, it was also noted that the number of features used for the neural network was too small, likely contributing to the poor reported accuracy.

It was noted analysing figure 17, that there was an apparent bias in the dataset towards class 1 (synchronised mu) activity. Re-examining the methodology used, there was an imbalance in the distribution of classes used in training, as two thirds of samples were taken from synchronised mu activity, seen in figure 7. As this apparent class imbalance was included in the training set, the support vector machine was biased in favour of class 1. To correct for bias, subsequent testing was performed, with an evenly balanced class distribution, with negligible changes in reported performance. Examining figures 13 and 16, it was noted that the synchronised mu activity

demonstrated a greater range of amplitudes, with the range of desynchronised μ values overlapping. As such, it was hypothesised that this may have caused the increased favourability of class 1 in both support vector machine and neural network classifiers.

Future Work

One major limitation with this study was the small dataset used for training both classifiers. By increasing the dataset available during training, reported performance could potentially be improved. As all participants tested noted fatigue from the protocol, extending the lengths of each session may not be reasonable, as this may lead to reduced participant performance. The use of subsequent sessions is another method that could increase the training dataset available. Furthermore, it would be valuable to investigate if additional training and familiarity with the protocol over subsequent sessions would improve participant performance in the motor imagery paradigm, potentially reducing reported BCI illiteracy.

Additionally, it would be interesting to test and compare different classifiers in the experimental protocol followed. Recent studies have demonstrated that convolutional neural networks can be used effectively in motor imagery tasks (Echtioui *et al.* 2023), with reduced network size allowing for faster convergence. Recurrent neural networks also offer an alternative classification method which has been shown to achieve comparable performance with convolutional neural networks (Ma *et al.* 2018). Since recurrent neural networks are perform particularly well in classifying temporally sequential datasets, they may be well-suited in real-time BCI.

Finally, by comparing figures 17 and 20 that the number of channels used in SVM training greatly impacts the resulting performance of the classifier. Future work should examine this relationship more closely, balancing the needs of BCI to rely on less electrodes, with the increased performance gained by using more channels. Ideally some minimum channel number can be determined such that classifier accuracy isn't significantly impacted.

PROJECT OUTCOMES

Conclusion

As part of chapter one, background information regarding neurodegenerative disorders and the current state of brain computer interfacing was provided to contextualise this project. For the project to be considered successful, a series of research questions were developed, with a complementary set of research objectives put forward to answer these questions.

Chapter two provided an overview of the current literature surrounding BCI research, with a particular emphasis on three key areas: sensory modality, experimental paradigm and classification technique used. From this literature review, a gap statement was produced to highlight a potential project for contribution to the literature. To that end, it was proposed that tCRE electrodes could be combined with a previously developed motor imagery paradigm that uses real and imagined movements. It was hypothesised that by utilising tCRE electrodes, noise artefacts could be reduced, resulting in improved classifier performance.

Chapter three detailed the methodology used in this project, subdividing it into three sections, focusing on data collection, the experimental protocol used, and the techniques used for classification. To achieve *RO1: Using a motor imagery paradigm, collect EEG data with tCRE*, data collection was performed using 13 tCRE electrodes connected to a CREmedical t-interface 20. As part of the classification phase, a support vector machine was trained on emulated EEG and tCRE data using LOSO cross-validation, satisfying *RO3: Develop a support vector machine classifier for comparing emulated EEG and tCRE performance with previous work*. A neural network classifier was included and trained using K-fold cross-validation, meeting the requirements for *RO4: Experiment with neural network classifiers for identifying event related desynchronisation*.

Chapter four highlighted the results of the project. Examining individual and group average graphs collected, decreased power of the mu frequency band could be observed in both emulated EEG and tCRE, answering *RQ1: Can event related desynchronisation be observed using tripolar concentric ring electrodes?*. To answer *RQ2: What differences can be observed in event related desynchronisation between tCRE and emulated EEG?*, a comparison was performed between emulated EEG and tCRE. It was noted that tCRE demonstrated less visual cohesion between electrodes, compared with emulated EEG. Examining the group average of the 'best-performing' electrodes used showed similarities in the desynchronisation measured between the two modalities, suggesting that tCRE does reduce mutual information and improve electrode selectivity.

Chapter five discussed the results of the project in the context of the literature. The performance of a support vector machine was compared between tCRE and emulated EEG, with an additional focus on results in similar studies. It was found that tCRE provided no additional benefit to classifier

performance, answering *RQ3: How does training an ERD classifier on tCRE data influence accuracy, in comparison to ordinary and emulated EEG?*. Similarly, examining the performance when training a neural network classifier yielded the same results; tCRE provided no add benefit to classifier performance, answering *RQ4: What differences in training performance can be observed between support vector machine and neural network algorithms?*. Classifier performance was notably lower than in the literature, suggesting alterations may be necessary to the methodology used. It was theorised that this discrepancy in performance is likely a result of only using a single electrode, which may remove too much information, rendering more accurate classification impossible. Retraining the support vector machine on all electrodes appears to confirm this, citing a higher accuracy. Future studies should investigate this further, minimising the number of electrodes used while maintaining comparably high performance.

BIBLIOGRAPHY

- Abiri, R. *et al.* (2019) 'A comprehensive review of EEG-based brain–computer interface paradigms', *Journal of Neural Engineering*, 16(1), p. 011001.
- Aghaei-Lasboo A *et al* (2020). Tripolar concentric EEG electrodes reduce noise. *Clinical Neurophysiology* [Online]. 131(1), pp 193-198.
- Aldea R and Fira M (2014). Classifications of motor imagery tasks in brain computer interface using linear discriminant analysis. *Journal of Advanced Research in Artificial Intelligence* [Online]. 3(7).
- Almajidy R *et al* (2015). A multimodal 2D brain computer interface. *Annual International Conference of IEEE Engineering in Medicine and Biology Society* [Online].
- Alzahrani, S. (2019) 'A comparison of tri-polar concentric ring electrodes to disc electrodes for decoding real and imaginary finger movements', *Colorado State University*
- Alzahrani S and Anderson C (2021). A comparison of conventional and tri-polar EEG electrodes for decoding real and imagined movements from one hand. *International Journal of Neural Systems* [Online]. 31(9).
- Amyotrophic lateral sclerosis (ALS)* (no date) *National Institute of Neurological Disorders and Stroke*.
- Balakrishnama S and Ganapathiraju A. Linear discriminant analysis – a brief tutorial. *Institute for Signal and Information Processing* [Online].
- Bell C *et al* (2008). Control of a humanoid robot by a noninvasive brain-computer interface in humans. *Journal of Neural Engineering* [Online]. 5(2), pp 214-220.
- Besio W *et al* (2006). Tri-polar concentric ring electrode development for Laplacian electroencephalography. *IEEE Transactions on bio-medical engineering* [Online]. 53(5), pp 926-933.
- Besio W *et al* (2008). Application of tripolar concentric electrodes and prefeature selection algorithm for brain-computer interface. *IEEE Transactions on Neural Systems and Rehabilitation Engineering* [Online].
- Besio W *et al* (2014). High-frequency oscillations recorded on the scalp of patients with epilepsy using tripolar concentric ring electrodes. *Journal of Translational Engineering in Health and Medicine* [Online].

- Bhattacharayya S et al (2011). Performance analysis of left/right hand movement classification from EEG signal by intelligent algorithms. *2011 IEEE Symposium on Computational Intelligence, Cognitive Algorithms, Mind and Brain* [Online]. Pp 1-8.
- Bian, Y. et al. (2018) 'Improvements in event-related desynchronization and classification performance of motor imagery using instructive dynamic guidance and complex tasks', *Computers in Biology and Medicine*, 96, pp. 266–273.
- Burianová, H. et al. (2013) 'Multimodal functional imaging of motor imagery using a novel paradigm', *NeuroImage*, 71, pp. 50–58.
- Burle B et al (2015). Spatial and temporal resolutions of EEG: is it really black and white? A scalp current density view. *International Journal of Psychophysiology* [Online]. 97(3), pp 210-220.
- Carvalhaes C and Barros J (2015). The surface Laplacian technique in EEG: theory and methods. *International Journal of Psychophysiology* [Online]. 97(3), pp 174-188.
- Chang M et al (2014). An amplitude-modulated visual stimulation for reducing eye fatigue in SSVEP-based brain-computer interfaces. *Clinical Neurophysiology* [Online]. 125(7), pp 1380-1391.
- Dose H et al (2018). An end-to-end deep learning approach to MI-EEG signal classification for BCIs. *Expert Systems with Applications* [Online]. 114(1), pp 532-542.
- Echtioui, A. et al. (2023) 'Convolutional neural network with support vector machine for motor imagery EEG Signal Classification', *Multimedia Tools and Applications* [Preprint].
- Fabiani M et al (1987). Definition, identification and reliability of measurement of the P300 component of the event-related brain potential. *Advances in Psychophysiology* [Online]. 2(3) pp 1-78.
- Farwell L and Donchin E (1988). Talking off the top of your head: toward a mental prosthesis utilizing event-related brain potentials. *Electroencephalography and Clinical Neurophysiology* [Online]. 70(6).
- Gil-González, I. et al. (2020) 'Quality of life in adults with multiple sclerosis: A systematic review', *BMJ Open*, 10(11).
- He B et al (2015). Noninvasive brain-computer interfaces based on sensorimotor rhythms. *Proceedings of the IEEE* [Online]. 103(6), pp 907-925.
- Jeunet, C. et al. (2016) 'Why standard brain-computer interface (BCI) training protocols should be changed: an experimental study', *Journal of Neural Engineering*, 13, p. 036024
- Kayser, J. et al. (2016) 'Issues and considerations for using scalp surface Laplacian in EEG/ERP research: a tutorial review', *International Journal of Psychophysiology*, 97(3), pp. 189-209

- Koka K and Besio W (2007). Improvement of spatial selectivity and decrease of mutual information of tripolar concentric ring electrodes. *Journal of Neuroscience Methods* [Online]. 165(2), pp 216-222.
- Lahr, J. *et al.* (2015) 'Invasive brain-machine interfaces: A survey of paralyzed patients' attitudes, knowledge and methods of information retrieval', *Journal of Neural Engineering*, 12(4), p. 043001.
- Lawhern V *et al* (2018). EEGNet: a compact convolutional neural network for EEG-based brain-computer interfaces. *Journal of Neural Engineering* [Online]. 15(1).
- Liu X (2013). Comparisons of the spatial resolution between disc and tripolar concentric ring electrodes. *Open Access Dissertations* [Online]. Paper 69.
- Liu X *et al* (2020). Improved spatial resolution of electroencephalogram using tripolar concentric ring electrode sensors. *Journal of Sensors* [Online].
- Ma, X. *et al.* (2018) 'Improving EEG-based motor imagery classification via spatial and temporal recurrent neural networks', *2018 40th Annual International Conference of the IEEE Engineering in Medicine and Biology Society (EMBC)* [Preprint].
- Makeyev O *et al* (2013). Multiple sensor integration for seizure onset detection in human patients comparing conventional disc versus novel tripolar concentric ring electrodes. *Annual International Conference of IEEE Engineering in Medicine and Biology Society* [Online].
- Michel C and Brunet D (2019). EEG source imaging: a practical review of the analysis steps. *Frontiers in Neurology* [Online]. 10(1).
- Müller S *et al* (2011). SSVEP-BCI implementation for 37-40 Hz frequency range. *Annual International Conference of IEEE Engineering in Medicine and Biology Society* [Online].
- Nicolas-Alonso, L.F. and Gomez-Gil, J. (2012) 'Brain Computer Interfaces, a review', *Sensors*, 12(2), pp. 1211–1279.
- Noble W (2006). What is a support vector machine? *Nature Biotechnology* [Online]. 24(1) pp 1565-1567.
- Ostendorf, P. (2022) 'Brain computer interface for neurodegenerative disease', *Flinders University*
- Piccione F *et al* (2006). P300-based brain computer interface: Reliability and performance in healthy and paralysed participants. *Clinical Neurophysiology* [Online]. 117(3), pp 531-537.
- Pfurtscheller, G. and Lopes da Silva, F.H. (1999) 'Event-related EEG/MEG synchronization and desynchronization: Basic principles', *Clinical Neurophysiology*, 110(11), pp. 1842–1857.
- Pfurtscheller G and Neuper C (1997). Motor imagery activates primary sensorimotor area in humans. *Neuroscience Letters* [Online]. 239(2-3).

- Polich J (2007). Updating P300: An integrative theory of P3a and P3b. *Clinical Neurophysiology* [Online]. 118(10), pp 2128-2148.
- Qiu, Z. *et al.* (2017) 'Optimized motor imagery paradigm based on imagining Chinese characters writing movement', *IEEE Transactions on Neural Systems and Rehabilitation Engineering*, 25(7), pp. 1009–1017.
- Sharma R *et al* (2022). Motor imagery classification in brain-machine interface with machine learning algorithms: Classical approach to multi-layer perceptron model. *Biomedical Signal Processing and Control* [Online]. 71(1).
- Talbott, E. O. *et al.* (2016) 'Chapter 13 – The epidemiology of amyotrophic lateral sclerosis', *Handbook of Clinical Neurology*, 138, p.225-238.
- Tang, T. K. (2021) 'Do tripolar concentric ring electrodes record sensorimotor rhythms better?', *Flinders University*
- Vialatte F *et al* (2010). Steady-state visually evoked potentials: Focus on essential paradigms and future perspectives. *Progress in Neurobiology* [Online]. 90(4), pp 418-438.
- Volosyak I *et al* (2011). BCI Demographics II: How many (and what kinds of) people can use a high-frequency SSVEP BCI. *IEEE Transactions on Neural Systems and Rehabilitation Engineering* [Online].
- Walton, C. *et al.* (2020) 'Rising prevalence of multiple sclerosis worldwide: Insights from the atlas of MS, Third edition', *Multiple Sclerosis Journal*, 26(14), pp. 1816–1821.
- Wang X *et al* (2020). An accurate EEGNet-based motor-imagery brain-computer interface for low-power edge computing. *IEEE International Symposium on Medical Measurements and Applications* [Online].
- Waytowich N *et al* (2018). Compact convolutional neural networks for classification of asynchronous steady-state visual evoked potentials. *Journal of Neural Engineering* [Online]. 15(6).
- Young, C.A. *et al.* (2021) 'Quality of life in multiple sclerosis is dominated by fatigue, disability and self-efficacy', *Journal of the Neurological Sciences*, 426, p. 117437.
- Zhang, R. *et al.* (2020) 'Subject inefficiency phenomenon of motor imagery brain-computer interface: Influence factors and potential solutions', *Brain Science Advances*, 6(3), pp. 224–241.
- Zhang Y *et al* (2019). Temporally constrained sparse group spatial patterns for motor imagery BCI. *IEEE Transaction on Cybernetics* [Online]. 49(9), pp 3322-3332.
- Zhao X *et al* (2022). Deep CNN model based on serial-parallel structure optimization for four-class motor imagery EEG classification. *Biomedical Signal Processing and Control* [Online]. 72(A).

APPENDICES

Appendix A

Check Desynchronisation Script

Script designed to take participant data and find the mean channel value for each time segment. The greatest difference in value signifies the greatest desynchronisation, which determined the appropriate channel used in training.

```
function check_desync(chan_info, target_channels)
    findindex = @(x,y) find(strcmp(x, y));
    chanselect = @(x,y) intersect(x,y);

    available_channels = fieldnames(chan_info);
    channels = chanselect(target_channels, available_channels);

    time_stamps = {-1, 0, 5, 10};

    highestDesync = 0;
    for i = 1:length(channels)
        chan = findindex(channels{i}, available_channels);
        chan_movements = fieldnames(chan_info.(available_channels{chan}));
        for move = 1:length(chan_movements)
            chan_mean = chan_info.(available_channels{chan}).(chan_movements{move}).mean;
            p_val = [];
            for T = 1:length(time_stamps)-1
                time_segment = chan_mean.selecttime(time_stamps{T}, time_stamps{T+1});
                p_val = [p_val, time_segment.meantime.data * ones(1, time_stamps{T+1} - time_stamps{T})];
            end

            if highestDesync < ((p_val(1)+p_val(3))/2)-p_val(2)
                highestDesync = ((p_val(1)+p_val(3))/2)-p_val(2);
                highestDesyncChan = available_channels{chan};
                highestDesyncMove = chan_movements{move};
            end

            subplot(length(chan_movements),1,move);
            plot(p_val, 'DisplayName', available_channels{chan});
            hold on
            if i == length(channels)
                legend show
            end
        end
    end
    end
    disp("=====");
    disp("highest desync value: " + highestDesync);
    disp(highestDesyncChan);
    disp(highestDesyncMove)
    disp("=====");
end
```

Appendix B

Class Rebalance Script

Since the number of samples belonging to each class was initially different, this script was designed to arbitrarily remove samples such that both class 1 and 2 datasets had the same number of samples

```
function out = create_even_class(observation_data, class_mapping)
    class0 = observation_data(class_mapping==0);
    class1 = observation_data(class_mapping==1);

    ix = randperm(length(class0), length(class0)-length(class1));
    class0(ix) = [];

    new_observation_data = [class0; class1];
    new_class_mapping = [zeros(size(class0)); ones(size(class1))];

    out = [new_observation_data, new_class_mapping];

end
```

Appendix C

Create Segments Function

Function designed to separate participant data into segments for creation of a training dataset

```
function [funcOut1, funcOut2] = create_segments(chan_info, target_channels, relative_out)
    findindex = @(x,y) find(strcmp(x, y));
    chanaelect = @(x,y) intersect(x,y);
    if ~exist('relative_out','var')
        relative_out = false;
    end
    available_channels = fieldnames(chan_info);
    %extracts desired channels from array of available channels
    channels = chanaelect(target_channels, available_channels);
    %segment duration in seconds
    segment_duration = 0.25;
    time_bounds = {-1, 10};
    class_mapping = [];
    %iterates through each channel
    for i = 1:length(channels)
        segment_list = [];
        chan = findindex(channels{i}, available_channels);
        %extracts the names of each movement within the channel struct
        chan_movements = fieldnames(chan_info.(available_channels{chan}));
        for move = 1:length(chan_movements)
            chan_move_samples = chan_info.(available_channels{chan}).(chan_movements{move});
            for j = 1:length(chan_move_samples)
                for seg = time_bounds{1}:segment_duration:(time_bounds{2}-segment_duration)
                    if relative_out == true
                        init_power = chan_move_samples(1).data;
                        init_power_value = init_power(1);
                    else
                        init_power_value = 1;
                    end
                    sample_segment = chan_move_samples(j).selecttime(seg, seg+segment_duration);
                    sample_segment.data = sample_segment.data/init_power_value;
                    segment_list = [segment_list, sample_segment];

                    if i == 1
                        if seg < 0 || seg > 5
                            class_marker = 0;
                        else
                            class_marker = 1;
                        end
                        class_mapping = [class_mapping; class_marker];
                    end
                end
            end
        end
        segment_out.(available_channels{chan}) = segment_list;
    end
    funcOut1 = segment_out;
    funcOut2 = class_mapping;
end
```

Appendix D

Training Dataset Creation Script

Creates a training dataset for use in a neural network by calling `create_segments` (Appendix C) and finding the mean for each time segment. Once complete a data is normalised and stored in a '.dat' file for use in training.

```
findindex = @(x,y) find(strcmp(x, y));
chanselect = @(x,y) intersect(x,y);

participants = { 'tP01', 'tP03', 'tP04', 'tP05', 'tP06', 'tP07', 'tP09' };
for parti = 1:length(participants)
    chan_info = chan_info_list(parti);
    available_channels = fieldnames(chan_info);
    %target_channels = {'CCP6h', 'CCP5h', 'FCC5h', 'CCP4h', 'FCC5h', 'FCC4h', 'CCP5h'};%tEEG_all;
    target_channels = {'tCCP6h', 'tFCC5h', 'tFCC5h', 'tCCP6h', 'tFCC5h', 'tCCP6h', 'tFCC4h'};
    %extracts desired channels from array of available channels
    channels = chanselect(target_channels, available_channels);

    [participant_segments, class_mapping] = create_segments(chan_info, target_channels{parti}, true);

    channel_data = [];

    for j = 1:length(participant_segments.(target_channels{parti}))
        chan_segments = [chan_segments, mean(participant_segments.(target_channels{parti})(j).data)];
    end
    channel_data = [normalize(chan_segments)];

    observation_data = transpose(channel_data);
    save_data = create_even_class(observation_data, class_mapping);
    address = "observation_data_"+ participants{parti}+"_tEEG.dat";
    save(address, 'save_data', '-ascii');
end
```